Comparison of Concrete Pavement Load-Stresses at AASHO Road Test with Previous Work

W. R. HUDSON,[1] Senior Designing Engineer, Highway Design Division, Texas Highway Department

Existing rigid pavement design equations spring primarily from the theories developed by Westergaard in 1925. Some of these design equations are based on empirical modifications of the original theory, others are merely simplifications. Several of the empirical modifications have been developed from strain measurements taken under static loads. Recent developments in electronic equipment allow more accurate dynamic strain measurement than was formerly possible. Such equipment was used to make approximately 100,000 individual strain gage readings under dynamic loads in conjunction with the AASHO Road Test (1958 to 1960).

The purpose of this paper is to discuss these strain measurements and to compare them with the static strain measurements used to develop existing empirical design equations. The stresses calculated from these strains will be compared with the original Westergaard theories. Such comparisons could provide the basis for modifying empirical design equations to include a dynamic load effect.

•THE primary results of the AASHO Road Test were performance equations relating pavement design, axle load, number of load applications, and pavement serviceability (1). These equations were developed with a great many other design variables held constant. Two methods will be helpful in analyzing these remaining variables to complete the general design equation: (a) additional road tests, and (b) development of a mechanistic model or equation relating the multitude of design variables. Judging from previous experience in structural research both approaches will ultimately be combined to provide the final solution of the problem.

This report is based on the idea that load-stresses offer an approach to a mechanistic model and that such a model will be helpful in extending the results of the AASHO Road Test equations.

It should be pointed out at this point that no stresses have been measured in this or any other study. Strains are measured and the corresponding stresses are calculated by use of elastic theory. Such stresses will be called "observed stresses" in this report. Theoretical stresses or those computed from empirical equations will be referred to as "calculated stresses." Symbols used in this report are defined where they first appear or where necessary for clarity, and for convenience in reference, are listed alphabetically in Appendix C.

EARLY HISTORY OF MATHEMATICAL AND THEORETICAL ANALYSES

In the early 1920's, A. T. Goldbeck and Clifford Older independently developed formulas for approximating the stresses in concrete pavement slabs under certain assumed conditions. The best known of these formulas is generally called the "corner formula" and is expressed

---

Paper sponsored by Committee on Rigid Pavement Design.

[1] Formerly, Assistant Chief, Rigid Pavement Research Branch, AASHO Road Test.

$$\sigma_c = \frac{3\,P}{h^2} \tag{1}$$

in which

σ_c = maximum tensile stress, psi, in a diagonal direction in the surface of the slab near a rectangular corner;
P = static load, in lb, applied at a point at the corner; and
h = depth of the concrete slab, in in.

Eq. 1 was derived using the assumptions of point load applied at the extreme corner and no support from the subgrade. The fiber stresses in the surface of the slab are assumed to be uniform on any section at right angles to the corner bisector.

Strain measurements taken on the Bates Road Test in 1922-23 appear to confirm the corner formula. Obviously, the assumptions of point load and load applied at the extreme corner were not correct for the Bates test sections. It is interesting that in spite of this there was reasonably good comparison. This good agreement could be partly due to the high impact transmitted to the slabs with the solid rubber tires used in the Bates test or to the possibility that subgrade support may have been very low as assumed by this formula.

In 1926, H. M. Westergaard completed a logical and scientific mathematical analysis of the stresses in concrete highway pavements. This analysis is concerned with the determination of maximum stresses in slabs of uniform thickness resulting from three separate conditions of loading:

1. Load applied near the corner of a large rectangular slab (corner load);
2. Load applied near the edge of a slab but at a considerable distance from any corner (edge load); and
3. Load applied at the interior of a large slab at a considerable distance from any edge (interior load).

In the solution of this problem, Westergaard made the following important assumptions:

1. The concrete slab acts as a homogeneous isotropic elastic solid in equilibrium.
2. The reactions of the subgrade are vertical only and they are proportional to the deflections of the slab.
3. The reactions of the subgrade per unit of area at any given point is equal to a constant k multiplied by the deflection at the point. This constant is termed "the modulus of subgrade reaction" or "subgrade modulus." The constant k is assumed to be constant at each point, independent of the deflection, and to be the same at all points within the area of consideration.
4. The thickness of the slab is assumed to be uniform.
5. The load at the interior and at the corner of the slab is distributed uniformly over a circular area of contact; for the corner loading, the circumference of this circular area is tangent to the edge of the slab.
6. The load at the edge of the slab is distributed uniformly over a semicircular area of contact, the diameter of the semicircle being at the edge of the slab.

The following expressions for stress were developed by Westergaard:

$$\sigma_i = 0.275\,(1+\mu)\,\frac{P}{h^2}\left(\log_{10}\frac{Eh^3}{k b^4}\right) \tag{2}$$

$$\sigma_e = 0.529\,(1+0.54\mu)\,\frac{P}{h^2}\left(\log_{10}\frac{Eh^3}{k b^4} - 0.71\right) \tag{3}$$

$$\sigma_c = \frac{P}{h^2}\left[1 - \left(\frac{12\,(1-\mu^2)\,k}{E\,h^3}\right)^{0.15}\ (a\sqrt{2})^{0.6}\right] \tag{4}$$

in which

P = point load, in lb;
σ_i = maximum tensile stress, in psi, at the bottom of the slab directly under the load, when the load is applied at a point in the interior of the slab at a considerable distance from the edges;
σ_e = maximum tensile stress, in psi, at the bottom of the slab directly under the load at the edge, and in a direction parallel to the edge;
σ_c = maximum tensile stress, in psi, at the top of the slab, in a direction parallel to the bisector of the corner angle, due to a load applied at the corner;
h = thickness of the concrete slab, in in.;
μ = Poisson's ratio for concrete;
E = modulus of elasticity of the concrete, in psi;
k = subgrade modulus, in pci;
a = radius of area of load contact, in in.; the area is circular in case of corner and interior loads and semicircular for edge loads;
b = radius of equivalent distribution of pressure at the bottom of the slab (= $\sqrt{1.6\,a^2 + h^2} - 0.675\,h$).

As a part of his analyses and in order to simplify further the discussions, Westergaard introduced a factor called the radius of relative stiffness ℓ, defined as

$$\ell = \sqrt{\frac{E\,h^3}{12\,(1-\mu^2)\,k}} \tag{5}$$

Eq. 4 can be expressed in terms of ℓ as follows:

Corner loading:

$$\sigma_c = \frac{3P}{h^2}\left[1 - \left(\frac{a\sqrt{2}}{\ell}\right)^{0.6}\right] \tag{6}$$

If μ is set at 0.15, Eqs. 2 and 3, respectively, may be expressed in the form:

Interior loading:

$$\sigma_i = 0.31625\,\frac{P}{h^2}\left[4\,\log_{10}\left(\frac{\ell}{b}\right) + 1.0693\right] \tag{7}$$

Edge loading:

$$\sigma_e = 0.57185\,\frac{P}{h^2}\left[4\,\log_{10}\left(\frac{\ell}{b}\right) + 0.3593\right] \tag{8}$$

Modifications to the original 1926 equations were made by Westergaard in 1933, 1939 and 1947. The 1933 modifications were concerned primarily with interior loads and will not be discussed in this paper.

In the 1930's, F. T. Sheets introduced an equation containing a constant c which was equated to the value of k as employed by Westergaard. The Sheets equation can be written as follows:

$$\sigma_c = \frac{2.4\ P\ (c)}{h^2} \tag{9}$$

Eq. 9 is reported to give stresses which are in good agreement with those obtained at the Bates Road Test; however, it is no longer in general use and does not contain all the variables of interest to the designer.

The principal weakness of these early stress equations was the rather broad assumptions necessary to facilitate analysis. Furthermore, with techniques available at that time it was difficult to make the strain measurements necessary to verify these stresses. As a result, very few stress comparisons were actually performed. Subsequent stress equations are all based on some modification of the original Westergaard equation. The major work that resulted in these modifications will be more completely discussed later in this paper, including the Kelley equation developed as a result of the BPR Arlington Test, the Spangler equation developed as the result of the Iowa State College tests and the Pickett equations developed as the result of additional mathematical analysis. Finally, the Maryland Road Test strain measurements will be discussed with the AASHO Road Test measurements in an effort to summarize all recent works in this field.

EFFECT OF PHYSICAL CONSTANTS

The values for physical constants assumed in calculation of theoretical stresses and in computation of observed stresses from measured strains can greatly influence the apparent correlations. For example, a variation of E from 4,000,000 to 5,000,000 psi results in an increase of 25 percent in the stresses computed from observed strain values. Such variations in E can exist and must be closely examined. The modulus of elasticity of the concrete can vary with age, moisture content, temperature and other factors. At best, any value used in computations must be an average value.

Aside from these variations in the "true" modulus of elasticity, the indicated modulus of elasticity as obtained from static load tests or dynamic (sonic) measurements vary greatly, with the dynamic value usually being 20 to 30 percent larger than the so-called static value.

Poisson's Ratio

Poisson's ratio μ is extremely hard to measure; however, it has only a minor influence on theoretical stresses or calculated observed stresses.

Modulus of Subgrade Reaction

The modulus of subgrade reaction k has no influence on calculated observed stress, but it can have significant influence on theoretical stress. Being a property of a granular material or soil, k inherently possesses all variations associated with such heterogeneous materials. For example, k varies with the density and moisture content of the material; with the temperature due to the curling characteristics of the slab; with the size of loaded area (plate size) used in the determination; and probably with the intensity of load due to the greater deflection imposed by higher loads.

It will be recalled that k is a stiffness coefficient that expresses the resistance of the soil structure to deformation under load in pounds per square inch of pressure per inch of deformation. Furthermore, the ability of a subgrade to maintain its k over the life of the pavement is extremely important. There are indications that most pavements have sufficient supporting power at the beginning of their life. However, as load appli-

cations are applied to the pavement, the character of the subgrade support changes until the pavement in many cases becomes relatively unsupported, particularly in the corner area. Common causes of this loss of support are pumping, settlement, and permanent deformation of the subgrade or subbase material. In addition to these variations inherent in the "true k value" there are variations dependent on the method of measurement used to determine k. A multitude of methods exist. The three basic methods are (a) calculation of k from the deflection of a rigid steel plate usually 30 in. in diameter (values of k have been found to vary with diameter), (b) calculations of k from measurements of load-deflection characteristics of existing slabs (13) and (c) assignment of k-value based on other soil strength tests, such as CBR, and triaxial compression tests.

ROAD TEST LOAD-STRESS EXPERIMENT

In conjunction with the AASHO Road Test (1958-1960) two major pavement strain measuring experiments were conducted: (a) edge strains on normal test pavements were measured under moving loads, and (b) a special factorial experiment was provided on a spacial no-traffic loop for measurement of strains under a vibrating load.

All concrete strains were measured with etched foil SR-4 strain gages. The effective gage length was 6 in. and the nominal gage resistance was 750 ohms. The sensitivity of the gages was ± μin. per in. of strain. The gages were cemented to the upper surface of the pavement slab and were protected from weather and traffic. Details of the measurement system are reported in the AASHO Road Test Report No. 5 (2).

In order to use these strain measurements to the best advantage, the gage readings were converted to principal strains, major and minor. These principal strains were converted to stresses by elastic theory. The development and formulas are given in Appendix E of Report 5 (2). In these conversions, Young's modulus E was taken equal to 6.25×10^6 psi, the dynamic modulus measured for concrete pavement at the Road Test. The static modulus for the Road Test pavement was 5.25×10^6 psi. Poisson's ratio μ was taken as 0.28, the average measured for the Road Test pavements (see Appendix A herein, and also Report 5, Appendix D, p. 284-286).

Main Loop Stresses

Measurement of Strains.—During the course of the project, 13 rounds of main loop strain data were gathered. A round consisted of one set of measurements on the selected factorial experiment, and the test vehicles normally assigned to a given lane were used as the test load for that lane (Fig. 1). Each round of strain data is representative of (a) the early morning pavement condition (pavement corners and edges curled up); (b) the period from 10:00 AM to 4:00 PM (pavements curled down); or (c) the period from 6:00 AM to 12:00 PM (pavements relatively flat). By varying this time of measurement, normal load-stress variations due to temperature differential within the slab could be studied. Several studies of pavement strain were also made continuously around the clock to provide more definitive information about strain variation with temperature differential.

No data from cracked slabs were used as a part of this experiment. Inspections were made to insure the uncracked condition of the slab being tested throughout the life of the project. When a crack occurred in the selected slab, a new slab was chosen and the gages relaid. When all slabs in a section cracked or a section was removed from the test, no further measurements were made on that section. Two gages were installed in each pavement section, one on each side of the joint (Fig. 2). Gages on 15-ft panels (nonreinforced section) were placed at the center of the panels, 7.5 ft from each joint. Gages on the 40-ft panels (lightly reinforced sections) were placed 10 ft from the joint. Output from the strain gages was recorded continously on paper tape as the test vehicles passed by. The strain value representative of one section for one round consisted of an average of 6 values, a minimum of 3 measurements on each of 2 strain gages. These measurements were made when the centroid of the loaded area (load wheels) was located opposite the gage and 20 in. (-3 to + 2 in.) from the pavement edge. (This biased tolerance was selected as the result of special studies of the distribution of the placement of

AASHO ROAD TEST

RIGID PAVEMENT
MAIN LOOP EXPERIMENT

Loop	Traffic Load	Subbase Thickness	Reinforcing	Surface Thickness 2.5 R	2.5 N	3.5 R	3.5 N	5.0 R	5.0 N	6.5 R	6.5 N	8.0 R	8.0 N	9.5 R	9.5 N	11.0 R	11.0 N	12.5 R	12.5 N
3	12k S	3				x	x	●	x	x	●	x	x						
		6				x	x	x	●	●	x	x	x						
		9				x	x	x	x	x	x	x	x						
	24k T	3				x	x	●	x	x	●	x	x						
		6				x	x	x	●	●	x	x	x						
		9				x	x	x	x	x	x	x	x						
4	18k S	3						x	x	●	x	x	●	x	x				
		6						x	x	x	●	●	x	x	x				
		9						x	x	x	x	x	x	x	x				
	32k T	3						x	x	●	x	x	●	x	x				
		6						x	x	x	●	●	x	x	x				
		9						x	x	x	x	x	x	x	x				
5	224kS	3								x	x	●	x	x	●	x	x		
		6								x	x	x	●	●	x	x	x		
		9								x	x	x	x	x	x	x	x		
	40k T	3								x	x	●	x	x	●	x	x		
		6								x	x	x	●	●	x	x	x		
		9								x	x	x	x	x	x	x	x		
6	30k S	3										x	x	●	x	x	●	x	x
		6										x	x	x	●	●	x	x	x
		9										x	x	x	x	x	x	x	x
	48k T	3										x	x	●	x	x	●	x	x
		6										x	x	x	●	●	x	x	x
		9										x	x	x	x	x	x	x	x

X Denotes a Test Section
● Denotes Replicate (2) Test Sections

Figure 1. AASHO Road Test, rigid pavement main loop experiment.

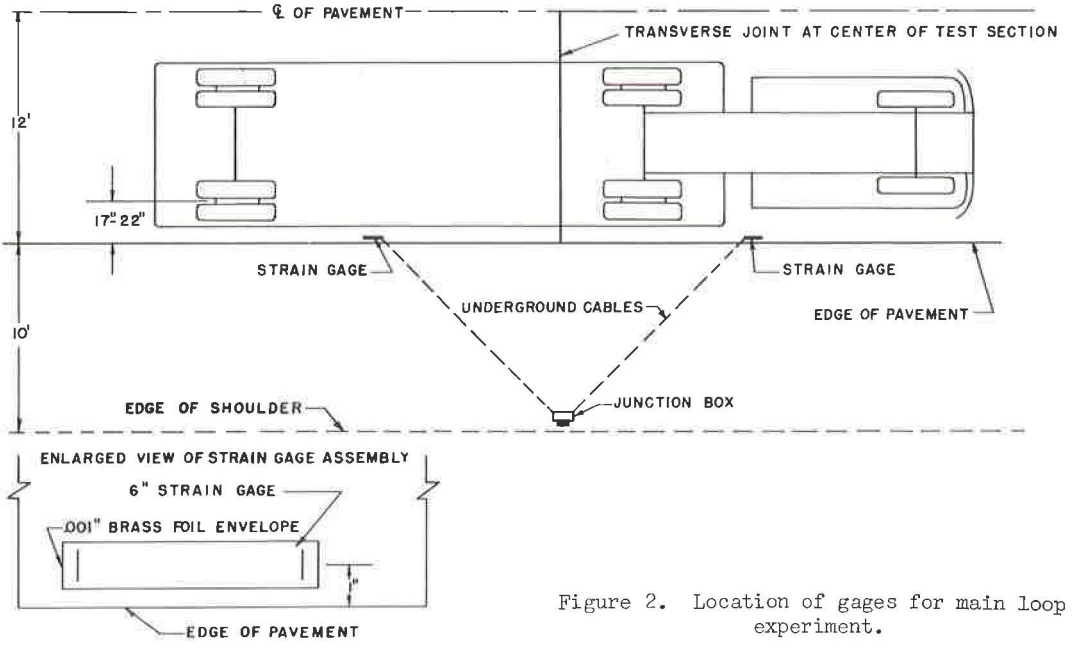

Figure 2. Location of gages for main loop experiment.

vehicles whose operators were attempting to drive at a specified distance of 20 in. from the pavement edge.) This placement resulted in the outer edge of the dual wheels being located at approximately 6 to 9 in. from the pavement edge.

Analysis of Data—Main Loops.—In early studies it became apparent that several variables should be isolated in order to simplify the study of strain data. Two of these variables were load and temperature.

Load Effects.—Several load-strain studies conducted early in the Road Test indicated that for a given pavement at a given time, strain varies linearly with load. This was substantiated many times. As a result of these studies the general mathematical model adopted for strains was

$$\frac{\text{strain}}{\text{axle load}} = f \text{ (design and other variables)} \tag{10}$$

Temperature Effects.—Strain measurements are affected by temperature. This was amply demonstrated early in the test. To isolate this variable, several 24-hr studies were made during the spring and fall seasons to take advantage of daily variation in ambient temperature. Numerous investigations of the data (strains, air temperatures, and internal slab temperature) indicated that a consistent variable for study was the temperature differential, top to bottom of a 6.5-in. thick PCC slab. These analyses led to the following model for best fit.

$$\frac{\text{strain}}{\text{axle load}} = f \text{ (design \& random variables)} \times 10^{f(\text{slab temp})} \tag{11}$$

General Strain Equation.—Dynamic edge strain data from Rounds 4, 5, 8, and 9, gathered between April and August 1959, were selected for use in determining the most representative empirical relationship between edge strain, design, load and temperature. These rounds cover spring, summer and fall seasons when a large majority of the sections were still in good condition.

Plots of the data and preliminary analyses along with load and temperature studies were helpful in selection of a model. The final analysis indicated that the design variables, reinforcing and subbase thickness, were not significant. The following equations resulted:

Single-axle loads:

$$\frac{\epsilon}{L_1} = \frac{20.54}{10^{0.0031T} D_2^{1.278}} \tag{12}$$

Tandem-axle loads:

$$\frac{\epsilon}{L_1} = \frac{3.814}{10^{0.0035T} D_2^{0.8523}} \tag{13}$$

in which

ϵ = estimated edge strain at the surface of the concrete slab;
L_1 = nominal axle load of the test vehicle (a single axle or a tandem-axle set);
D_2 = nominal thickness of the concrete slabs; and
T = the temperature (° F) at a point ¼ in. below the top surface of the 6.5-in. slab minus the temperature at a point ½ in. above the bottom surface, determined at the time the strain was measured (the statistic T may be referred to occasionally as "the standard differential").

Residuals from the analyses that are less than the average root mean square residual determined in the two analyses correspond to observations that range from 83 to 120 percent of the predicted values.

Using the theory of elasticity given in Report 5, Appendix E (2), Eqs. 12 and 13 were converted to the following stress equations:

Single-axle loads:

$$\sigma_{es} = \frac{139.2L_1}{10^{0.0031T} D_2^{1.278}} \tag{14}$$

Tandem-axle loads:

$$\sigma_{et} = \frac{25.86L_1}{10^{0.00335T} D_2^{0.8523}} \tag{15}$$

in which

σ_{es} = predicted stress under single-axle load; and
σ_{et} = predicted stress under tandem-axle load.

L_1, T, and D_2 are as previously described.

Special No-Traffic Loop Stresses

Between October 9, 1959, and November 2, 1960, a series of eight experiments, designed to furnish information regarding the distribution of load stress in the surface of concrete slabs, was conducted on the sections comprising the experiment on the no-traffic loop (Table 1).

A rapidly oscillating load was applied to the pavement through two wooden pads on 6-ft centers, each approximating the loaded area of a typical dual tire assembly loaded to 22.4^k (Fig. 3). This dynamic loading was intended to simulate that of a typical single-axle vehicle used in the main loop experiments.

Dynamic Load.—The vibrating loader was mounted on a truck (Fig. 4). The essential parts were two adjustable weights rotating in opposite directions in a vertical plane in such a manner that all dynamic force components except those in a vertical direction were balanced by equal and opposite components. The deadweight necessary to prevent the upward components from lifting the truck from the pavement was provided in the form of concrete blocks resting on a platform located directly above the rotating weights.

TABLE 1

EXPERIMENT DESIGN FOR SPECIAL STUDIES OF LOAD STRESSES IN THE SURFACE OF CONCRETE SLABS

Subbase Thickness (in.)	No. of Sections					
	5.0-In. Slab, 12,000-Lb Load		9.5-In. Slab, 22,000-Lb Load		12.5-In. Slab, 30,000-Lb Load	
	No Reinf.	Reinf.	No Reinf.	Reinf.	No Reinf.	Reinf.
0	2	1	1	2	2	1
6	2	1	1	2	2	1

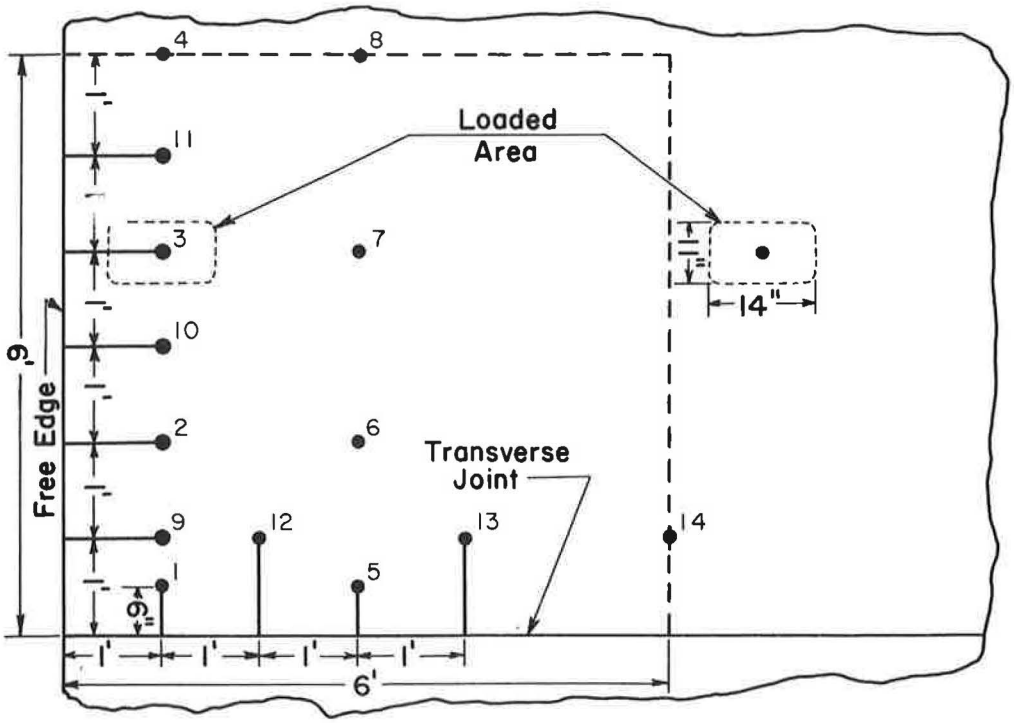

Figure 3. Load positions for special strain studies.

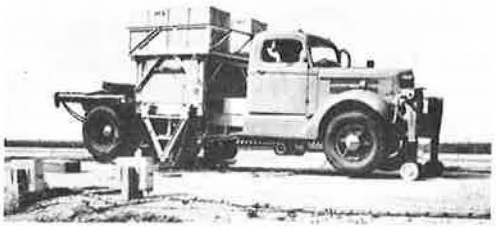

Figure 4. Truck-mounted vibrator in position on pavement.

The load was transmitted through inverted A-frames which could be folded upward against the side of the vehicle when not in use. Contact with the pavement being loaded was solely through the wooden pads.

During each of the eight experiments (rounds), the simulated single-axle load was applied at three or more of the positions indicated in Figure 3. Data from Round 7, taken in September 1960 during the early morning hours when panel corners were curled upward and the strains were among the highest observed, were selected for complete analysis and are presented in the Road Test report and used herein. Other data are available in Road Test file, DS 5205.

Field Procedures.—Strains were measured by means of 33 electrical resistance strain gages cemented to the upper surface of the pavement slab. The gages were laid out over the corner 6-sq ft area of the slab in each section (Fig. 5).

The use of delta rosettes at the 9 interior points permitted the computation of the magnitude and direction of the principal strains at those points. Only single gages were used along the edge and transverse joint, it being assumed that the strain perpendicular to the edge or joint could be calculated by use of Poisson's ratio for the concrete. No gages were required at the intersection of joint and edge as the strain there was assumed to be zero. Figure 6 shows the points at which gages were assumed to act.

Load cells for measuring the vibratory loads were developed at the project and were calibrated on the project's electronic scales. A continuous record of loading was made while the strain gage output was being recorded.

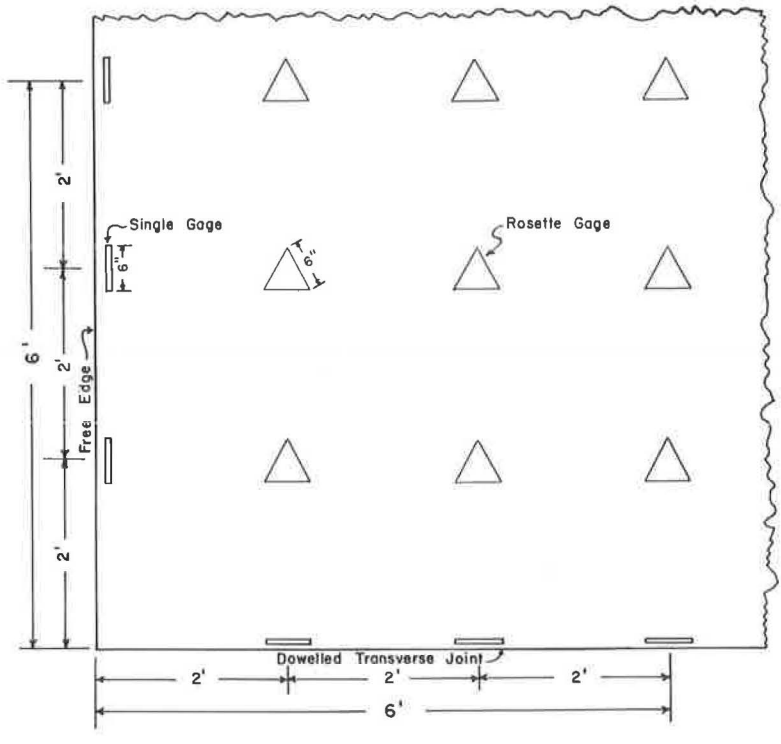

Figure 5. Typical gage layout, no-traffic loop strain experiment.

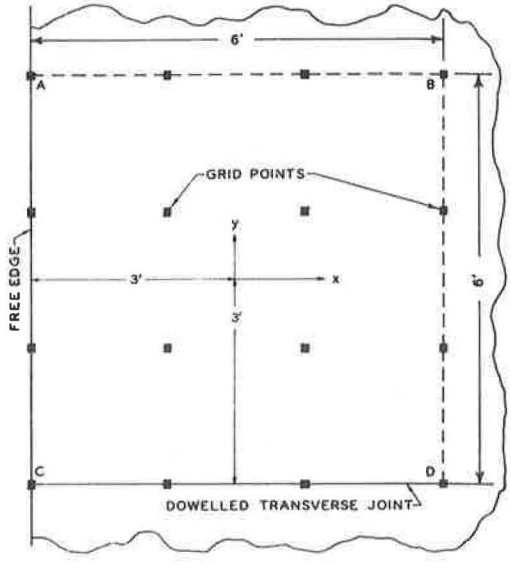

Figure 6. Control points for special strain studies.

In normal operation, the load was varied sinusoidally with time at a frequency of 6 cps, from a minimum value of about 500 lb on each contact area to a maximum value which depended upon the thickness of the pavement being tested (Table 1). The measured strain also varied sinusoidally with time, very nearly in phase with the load, and of course, at the same frequency. From examination of simultaneous traces of the load wave and strain wave it was possible to determine the amplitude of each as well as the nature (tension or compression) of the strain.

Data Collection.—Data were taken on the test sections in random order within the experiment. All load positions selected for a particular round were completed on a section before measurements were made on the next section. With the load in one of the selected positions, the recording equipment was switched to each of the 33 pavement gages in succession. The output of each pavement gage was recorded on paper tape, along with the record from the load gages. The overall time required to

complete the measurements associated with one load position on one section, including the time required to set up the vibrating loader, was about 30 min, of which about 5 min were spent in recording the strains.

Data Processing.—The first requirement for each experiment was to derive by statistical techniques a pair of empirical equations for each load position, of the following general forms:

$$\text{Major principal strain} = \text{a function of pavement design, load and the coordinates of the gage point} \quad (16)$$

$$\text{Minor principal strain} = \text{a function of pavement design, load and the coordinates of the gage point} \quad (17)$$

(The coordinate system used was that shown in Figure 6.)

The second requirement was to compute from Eqs. 16 and 17, and the appropriate plane stress equations linking stress and strain, the estimated value of major and minor principal stresses at closely spaced points in the pavement surface within the 36 sq ft area of observation.

Examination of the data indicated that variations in the strain observed on sections at the same level of slab thickness but at different levels of reinforcing and/or subbase thickness were small and apparently random in nature. Therefore, within each round and for the same load position, the readings of gages with the same coordinates x and y installed on panels of the same slab thickness (irrespective of subbase thickness and reinforcing) were averaged to obtain a set of data representing the round-load position-slab thickness combination.

Thus, for one load position within an experiment, the processing resulted in three sets of data corresponding to the three levels of slab thickness (5.0, 9.5, and 12.5 in.) with each set consisting of 33 averaged strain gage readings. As the third step in processing, each such set was converted from strain gage readings to magnitude and direction of major and minor principal strains at the 15 gage points on a panel employing standard techniques based on elastic theory.

As the fourth and final step before analysis, each principal strain was divided by the corresponding load in accordance with experimental evidence (as described herein) that strain is directly proportional to load. Thus, as a result of the four-step processing of the data, the only remaining independent variables to be considered in the analysis of strain were the coordinates x and y of a gage point and the thickness D_2 of the slab.

Typical Stress Distribution Results.—Analysis of Strains.—The three sets of data corresponding to each round-load position combination were analyzed using statistical procedures. The strain data were represented by a linear model whose 48 terms (3 slab thicknesses by 16 combinations of x and y) were mutually orthogonal polynomials in x, y, and D_2. As a result of the elimination of reinforcing and subbase thickness as independent variables, there were 6 sections within each round-load position-slab thickness combination whose variation in strain furnished a measure of residual effects. The residual effects, in turn, were used to determine the statistical significance of each coefficient. (The coefficients from each analysis, with significant terms indicated, are available in Road Test file DS 5211.) Of the 48 original coefficients only those that were found to be significant at the 1 percent level were used in the calculations to be described below.

Distribution of Principal Stresses.—As previously indicated, the analyses of data from load positions 1, 2, 3, and 4 of Round 7 were selected for complete study. The stresses determined were used in plotting contours of equal principal stress (see Fig. 9). In these plots all stresses are recorded in pounds per square inch with the usual sign convention—tensile stresses positive, compressive stresses negative.

Critical Stresses (Edge Load Condition).—Maximum values of tensile stresses and maximum values of compressive stresses for the edge load positions studied were taken

TABLE 2

MAXIMUM TENSILE AND COMPRESSIVE STRESSES FOR 1-KIP SINGLE-AXLE LOAD
(Data from Design 1, Loop 1, Lane 2)

Load Position	Slab Thickness (in.)		
	5.0	9.5	12.5
(a) Maximum Tensile Stress, psi			
1	12.47	4.21	2.62
2	9.39	3.27	2.05
3	8.58	2.85	1.38
4	6.94	2.60	1.52
(b) Maximum Compressive Stress, psi			
1	- 3.78	-1.61	-1.12
2	-17.97	-7.41	-4.71
3	-18.82*	-7.82	-4.89
4	-17.57	-8.10*	-5.57*

*Maximum for indicated slab thickness.

from Figure 7 and recorded in Table 2. Figure 7 shows the load position and the stress distribution when these critical stresses occurred.

According to an assumption commonly made in the application of elastic theory to a slab resting on an elastic foundation (4), the stresses at points on a vertical line through the slab are equal but opposite in sign at the slab surfaces and exceed, in absolute value, the stress at any other point on the line. If this assumption is made in the present instance, then each stress marked with an asterisk in Table 2 is equivalent, in absolute value, to the critical tensile stress for the indicated slab thickness and load position. These stresses occur along the pavement edge with the center of the outer loaded area at a distance of 1 ft from the edge and 4 to 6 ft from the nearest transverse joint (edge load conditions).

The following empirical equation is fitted to the three pairs of values of D_2 and critical stress given in Table 2.

$$\sigma_{ev} = \frac{160 L_1}{D_2^{1.33}} \tag{18}$$

in which

σ_{ev} = the critical load stress, in psi, as determined under a vibratory load on the no-traffic loop (edge load);
L_1 = single-axle load, in kips; and
D_2 = slab thickness, in in.

or in terms of wheel load (L_W):

$$\sigma_{ev} = \frac{320 L_W}{D_2^{1.33}} \tag{19}$$

Eq. 18 (Fig. 8) predicts the three critical stresses denoted by asterisks in Table 2 with an error of less than 2 percent. The critical load stress for any combination of single-axle load and pavement thickness, within the range observed, presumably may be estimated from Eq. 18. Additional stresses which may be present as a result of temperature or moisture fluctuations, of course, are not included in the stress estimated from this curve or from the contours (Fig. 7). It is also probable that stresses arising from static loads would be greater than those estimated from the strains measured in this study.

Stress Distributions for Corner Loading Conditions.—Previous research has indicated that the corner loading condition is of considerable importance in the study of pavement behavior. To provide a basis for comparison with previous data for this case of loading, the results of the corner load position of the Loop 1 strain experiments are

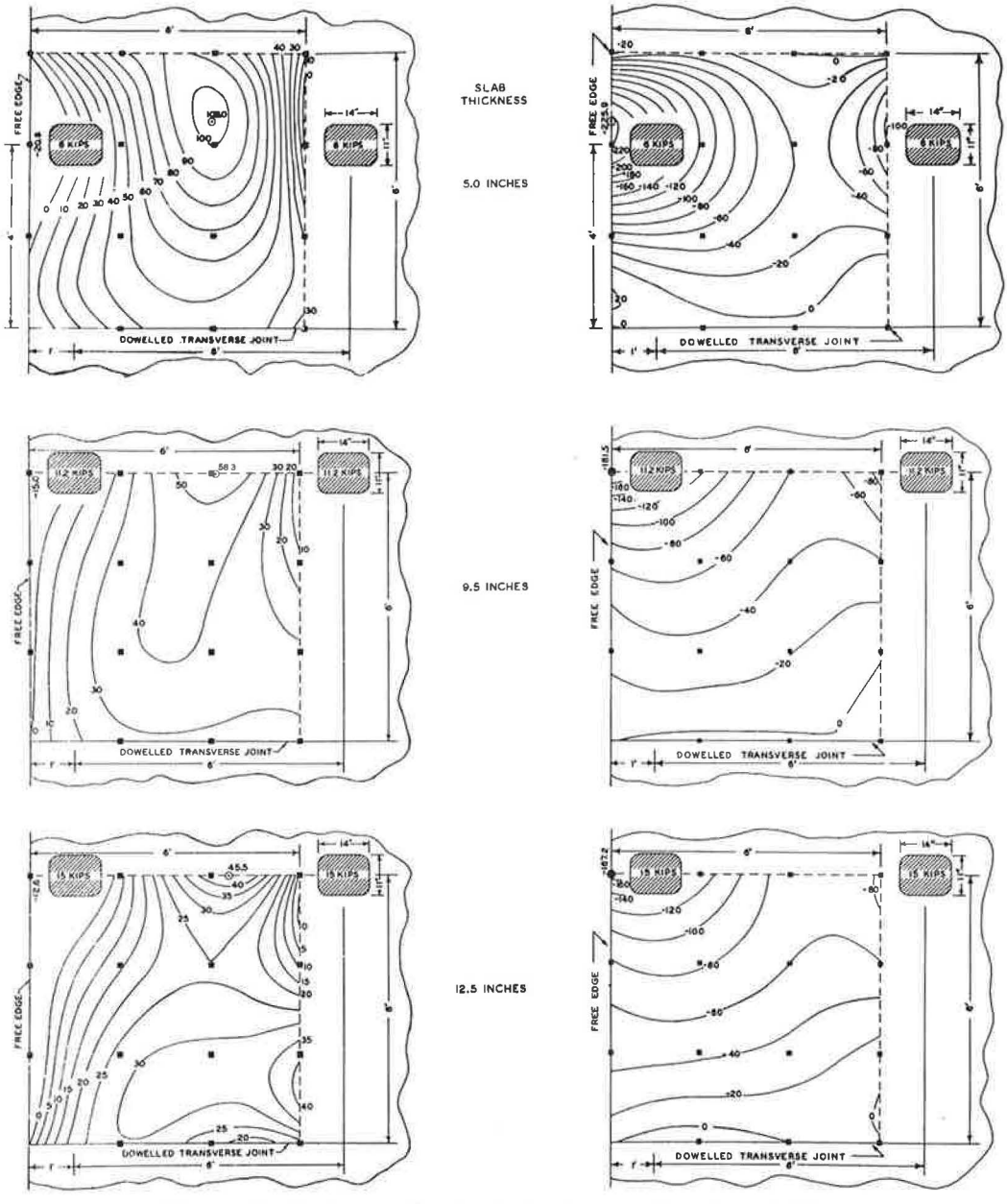

Figure 7. Contours of principal stresses for edge studies.

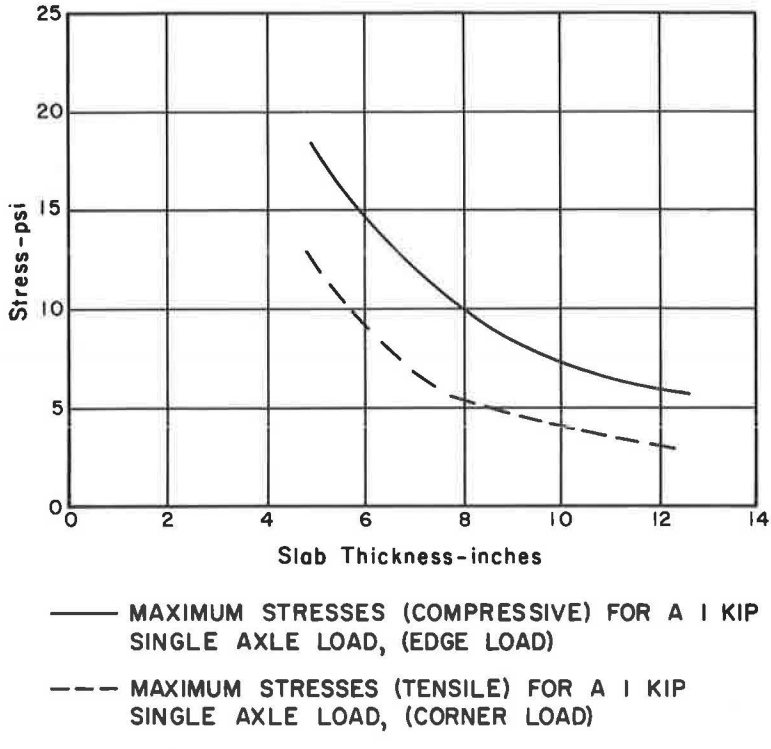

Figure 8. Plot of AASHO Road Test stress equation.

given in Figure 9; the directions of the principal stresses are given in Figure 10. These stress directions have not previously been reported although the stress contours are part of the Road Test reports.

Maximum stresses indicated for corner loading can be obtained from Figure 9. Using these values a corner stress equation can be developed exactly as Eq. 18 was developed for edge loading.

$$\sigma_{cv} = \frac{193 L_1}{D_2^{1.7}} \tag{20}$$

in which

σ_{cv} = maximum load stress, in psi, as determined in Loop 1 for corner load.

L_1 and D_2 are as previously defined. In terms of wheel load L_W this equation becomes

$$\sigma_{cv} = \frac{386 L_W}{D_2^{1.7}} \tag{21}$$

(Eq. 20 is also shown in Figure 8.)

Comparison of Main Loop and No-Traffic Loop Stresses

The use of dynamic loaders (such as the vibrator used in the no-traffic loop) in future experiments would facilitate the study of pavement strains under dynamic load conditions However, such studies will be useful only if the stresses observed under this dynamic

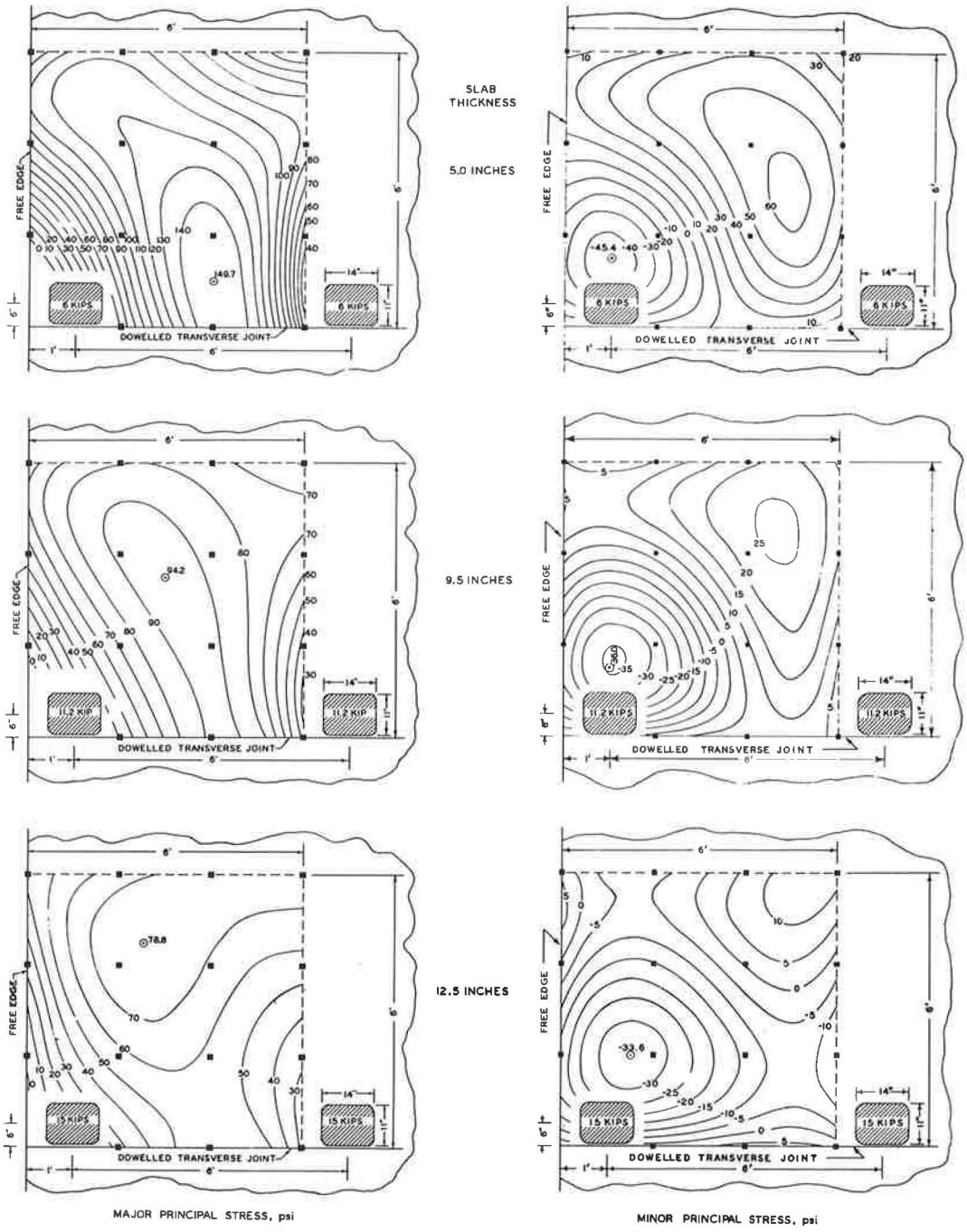

Figure 9. Contours of principal stress for corner load.

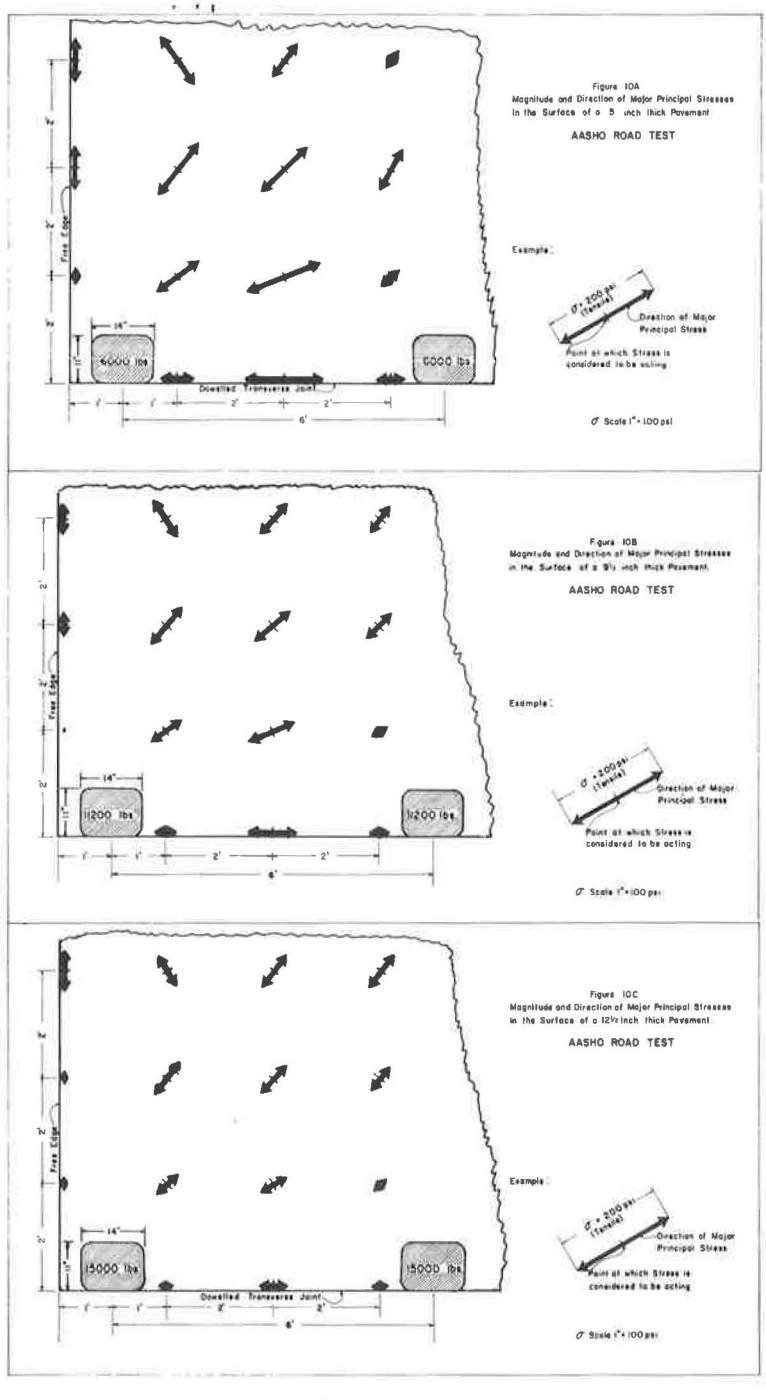

Figure 10. Magnitude and direction of major principal stresses.

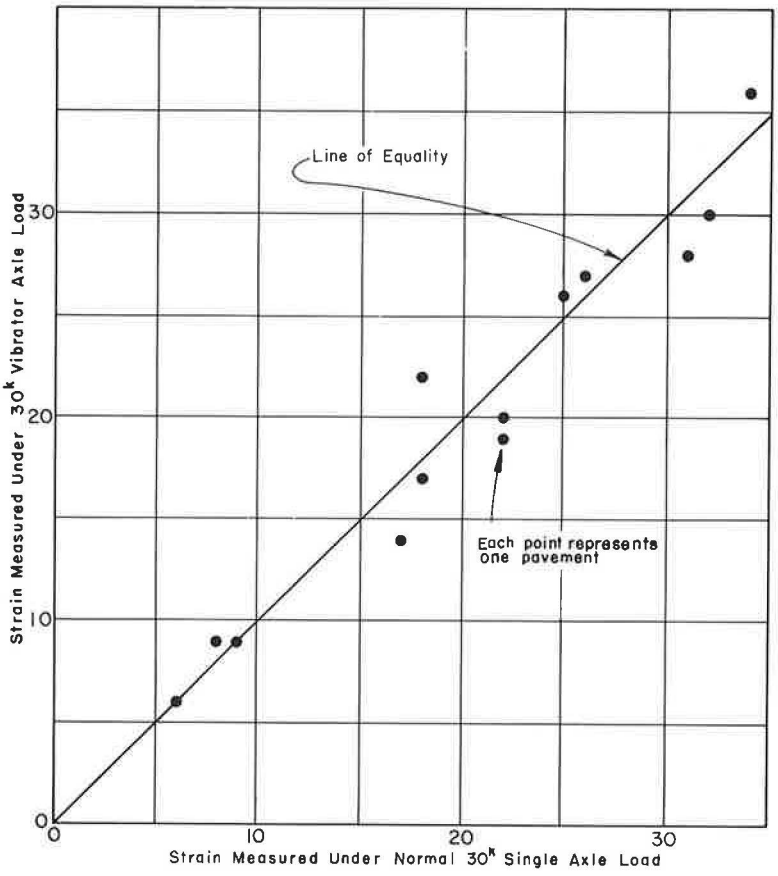

Figure 11. Correlations of vibratory loads and normal load.

loading device are comparable to stresses under normal traffic. It seems reasonable to compare the stress equations obtained for the two loading conditions to evaluate this device. It is also desirable to compare the observed stresses for selected pavement slabs under both routine truck traffic and the vibrator loaded to the same axle weight.

Figure 11 indicates that strains measured under a normal 30-kip single-axle vehicle and a 30-kip vibratory load are substantially equal.

If T is made equal to zero the main loop equation for edge stresses under single-axle loads (Eq. 4) becomes

$$\sigma_{es} = \frac{139.2\ L_1}{D_2^{1.278}} \tag{22}$$

Eq. 22 gives stresses nearly equal in value to those computed from the Loop 1 critical edge stress equation (Eq. 18) as shown in Figure 12. When D is 11 or 12.5 in., the stresses are numerically equal. The difference between these two equations could be due to one or more of the following reasons among others:

1. σ_{ev} are maximum stresses and their location varies with slab thickness, whereas σ_{es} is calculated for a fixed edge location.

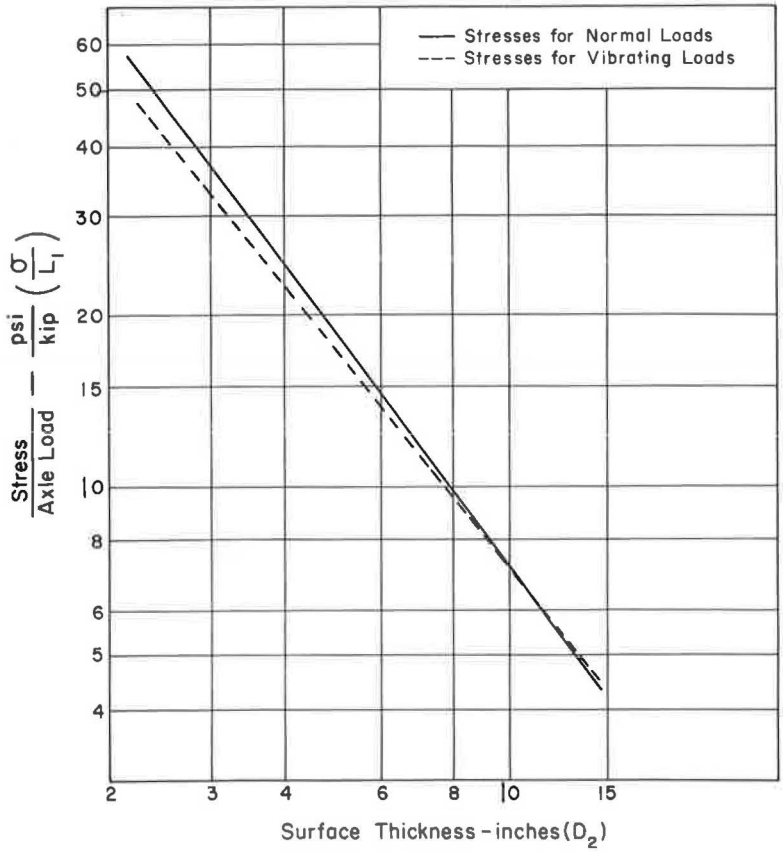

Figure 12. Comparison of normal load and vibratory load edge stress equation.

2. The loads used to induce σ_{ev} were applied through a wooden contact area of fixed size; σ_{es} were induced by normal tires and in general the contact area increased with slab thickness.

3. Both σ_{ev} and σ_{es} occurred with the load near the pavement edge; however, the centroid of the loaded area was slightly closer to the location of σ_{ev} than to the location of σ_{es}.

This close agreement between these stress equations supports the thesis of using the dynamic loader for future experiments with dynamic stresses.

PREVIOUS THEORETICAL AND EXPERIMENTAL WORK

This section compares the AASHO Road Test strain experiments with the theoretical equations developed by Westergaard, as well as the observed stresses and the resulting empirical equations from:

1. Bureau of Public Roads Tests conducted at Arlington, Va., 1933 to 1942, by Bureau of Public Roads' personnel and reported by Teller and Sutherland (4). Equation was developed and reported by Kelley (9).
2. Iowa State College Tests conducted indoors, 1930 to 1938, by Spangler (5).
3. Maryland Road Test, strain measurements made on the Maryland Road Test pavements 1950 (12) Highway Research Board Special Report 4.
4. Pickett Equation, mathematical work done by Pickett (11) in an effort to make an empirical equation which has rational boundary conditions as well as fit observed data previously reported by others.

These comparisons and analyses are broken into four categories: corner load conditions, edge load conditions, miscellaneous comparisons, and general overall comparisons. Necessary descriptive data relative to comparisons with the Road Test data are given.

Bureau of Public Roads' Arlington Tests

In 1930, the BPR began a research project, a portion of which had as its objective, "a study of the deflections, strains, and resulting stresses caused by highway loads placed in various positions on concrete slabs of uniform thickness." The data obtained from this project were analyzed using Westergaard's 1926 equations primarily.

Description of the Project.—Concrete Pavement.—The investigation was carried out on 10 full-size concrete pavement slabs especially constructed near Arlington, Va. Each of these slabs was 40 by 20 ft overall, divided by 1 longitudinal and 1 tranverse joint to produce 20-by 10-ft panels. Each slab was separated from those adjoining it by a 2-in. open joint. Slabs of uniform thickness of 6, 7, 8, and 9 in. were constructed. All slabs were nonreinforced (plain concrete). The static modulus of elasticity for concrete control specimens after 12 months' storage in a normal laboratory atmosphere averaged 4,500,000 psi for summer conditions and 5,500,000 psi for winter conditions. Poisson's ratio was assumed to be 0.15. Coarse aggregate was $1\frac{1}{2}$-in. maximum size limestone. The concrete was proportioned to provide an average 28-day flexural strength of 765 psi. The average compressive strength at 28 days was 3,525 psi.

Subgrade Conditions.—The supporting soil for the slabs was a uniform brown, silty loam, Class A-4. The subgrade was plowed to a depth of about 10 in. before construction of the slab. After remaining in this loose condition for several weeks it was compacted with a 5-ton tandem roller followed by a loaded 5-ton motor truck. Daily sprinkling was provided during construction to maintain a uniform moisture content. The soil had a liquid limit of 25, a plasticity index of 9, a shrinkage limit of 19, and a shrinkage ratio of 1.8.

Testing Procedures.—Loading Procedures.—For the corner and interior loading conditions circular metal bearing plates with 6-, 8-, 12-, 16-, and 20-in. diameters were used. For edge loadings the bearing plates were semicircular with the diameter acting at the slab edge. Static loads were applied through a jack and reaction loading system. It was found that from 1 to 5 min of load application was required to "develop maximum stress." Therefore, all loads were applied for 5 min with a recovery period of at least 5 min between loads. This long loading period should be kept in mind when these observed stresses (strains) are compared with stresses observed under normal momentary dynamic loads. Loads of 7,000, 9,000, 12,000 and 15,000 lb were applied, respectively, to the 6-, 7-, 8-, and 9-in. pavement slabs. These loads created maximum stresses which approximated one-half of the modulus of rupture of the concrete.

Determination of Modulus of Subgrade Reaction.—Westergaard's original equations involve a coefficient of subgrade stiffness k called the subgrade modulus. To make practical use of the Westergaard equations, it is necessary to assign a value to this subgrade modulus for the conditions prevailing during the test. At the time of this particular investigation no determinations of the value of such a soil coefficient had been made. There was, therefore, no previous experience to indicate either the probable range of values of coefficients or a procedure by which values might be obtained. It was decided, however, that the factor used should simulate the action of a loaded slab. As a part of this experiment, tests were made to develop a proper testing procedure for determination of k. The procedure selected was that of loading a 30-in. diameter steel plate on the subgrade until a deflection of 0.05 in. was reached. Unit load required to produce this deflection was divided by 0.5 in. resulting in the coefficient k in pounds per square inch per inch of deflection.

It is important to note at this point that the k value used by the Bureau of Public Roads in its analysis of this test was not derived from the described plate bearing test. Instead k was determined by substituting the observed deflection of a loaded slab in the theoretical equation for maximum deflection and solving the equation for the value of k. In general a pavement design would not have the advantage of this method of evaluating k and other correlating methods must be developed.

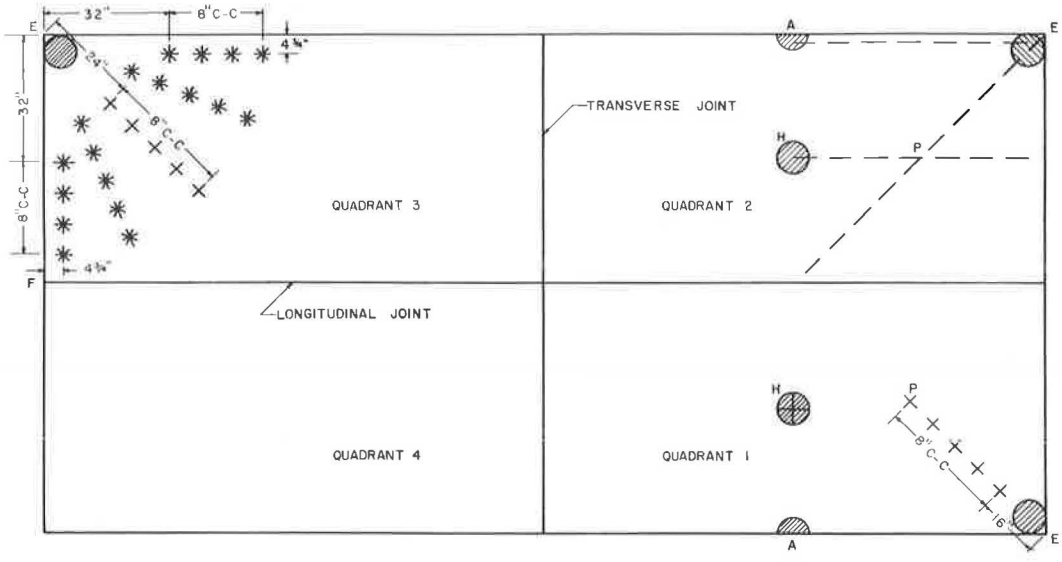

CIRCLES AND SEMI-CIRCLES SHOW POSITIONS AT WHICH LOADS WERE APPLIED.
CROSSES (QUADRANTS 1 AND 3) AND ROSETTES (QUADRANT 3) SHOW STRAIN GAGE POSITIONS.
DASH LINES (QUADRANT 2) SHOW LINES ALONG WHICH DEFLECTIONS WERE MEASURED.

Figure 13. Plan of BPR test slab.

Strain Measurements and Stress Determinations.—Strain Measurements.—Strains were measured with a temperature compensating recording strain gage approximately 6.6 in. in length installed between metal plugs set in the top surface of the concrete slab. To evaluate the bottom strains it was assumed that the strain in the bottom of the slab was equal to the strain in the surface of the slab directly above it though opposite in sign. The assumption has previously been substantiated. Teller reported that in one test series the recording strain gages were attached to both bottom and top of a concrete slab which was supported on the ends only. Equal and opposite strains were recorded at both slab faces when load was applied. Additional research into this point would be very helpful because some tests at very high loads indicate a shift in the neutral axis of the slab with a resulting differential in the strain at top and bottom. However, the assumption of equal strains top and bottom is common to all the tests discussed in this paper. An example slab showing locations of applied load and arrangement of strain gages is shown in Figure 13.

Stress Determinations.—The measured strains were converted to stress by the use of elastic theory. The equations used are the same as those reported in Report 5, Appendix E, p. 290 for the Road Test measurements.

Iowa State College Tests

About 1930, research was begun at Iowa State College in an attempt to study corner stress conditions. The primary purpose was to provide experimental data for verification or modification of the original corner equation and the Westergaard corner equation for the design of concrete pavement slabs.

Description of the Project.—Concrete Pavement.—Five experimental slabs were constructed in a basement laboratory to provide controlled conditions for testing. Slab 1 was used primarily for development of procedure and measuring techniques. Details of the remaining slabs are given in Table 3. In the study of these slabs, slight tipping of the corner opposite the load was noted, but this was assumed to be negligible by the original author.

TABLE 3

PHYSICAL CHARACTERISTICS AND DIMENSIONS OF TEST SLABS[a]

Slab	Date Const.	Date Tested	Size (ft)	Thickness (in.)	W/C Ratio (by wt.)	Moist Curing	Avg. Properties of Control Specimens at Time Tested			
							Compression (psi)	Modulus of Rupture (psi)	Modulus of Elasticity (psi)	Poisson's Ratio
2	1932	1932-33	10 × 12	6	0.80	Earth	4,400	650	3,750,000	—
3	6/18/35	7/5 to 9/20/35	10 × 12	6	0.80	Burlap	3,300	520	2,270,000	0.20
4	6/24/36	7/15 to 8/15/36 1/9 to 2/23/37	12 × 12	6	0.75	Burlap	4,700	680	4,000,000	0.25
5	6/2/38	7/8 to 8/8/38	12 × 12	4	0.80	Burlap	3,080	490	2,430,000	0.23

[a] No reinforcement; high-early strength cement; limestone coarse aggregate; mix, by weight, 1:1.4:4; control specimens were beams and cylinders.

Subgrade. — The subgrades for the experimental slabs were constructed by tamping moist, yellow, clay loam in thin layers within a 12- by 14-ft wooden crib for slabs 2 and 3, and a 14- by 14-ft crib for slabs 4 and 5. All the subgrades were 2-ft thick above the concrete floor. Values of k, subgrade modulus, were assigned by dividing the unit load at any point within the slab by the deflection of the slab at that point. For analysis, the value of k was taken to be 100. Spangler reports that under the slab the value of k decreases as the radial distance from the corner increases. For example, under slab 5, k varied from 650 psi per in. at the corner to about 50 psi per in. at a distance of 40 in. from the corner. This is not consistent with the original Westergaard assumption that k is considered uniform at every point under the slab. Westergaard later reports, however, that k probably varies under the slab with the deflection.

Load Procedures. — Static loads were applied to slabs through a circular cast-iron 6.72-in. diameter bearing plate. A cushion of corn-stalk insulation board was used between the plate and the slab to help distribute the load uniformly over the circular area. Loads were measured with a pair of calibrated springs mounted between two cast-iron plates. Load magnitudes are given in Table 4.

Stress Determinations. — Strains were measured by means of optical levered extensometers approximately 3 in. long. These extensometers were placed in a rosette pattern and provided data for calculation of the maximum and minimum principal strains by graphical construction. These principal strains were then converted to stresses by the equations given in Report 5, Appendix E (2).

Maryland Road Test Strain Measurements

During the last six months of 1950, controlled traffic tests were run over a 1.1-mi section of PCC pavement constructed in 1941 on US 301 approximately 9.0 miles south of LaPlata, Md. The pavement consisted of two 12-ft lanes each having a 9-7-9-in. cross-section and reinforced with wire mesh. Expansion joints were spaced at 120 ft intervals with 2 intermediate contraction joints at 40 ft spacings. All transverse joints had ¾-in. diameter dowels on 15-in. spacing, and the adjacent lanes were tied together with tie bars 4 ft long spaced at

TABLE 4

LOAD VALUES USED IN IOWA STATE TESTS

Slab	Loads for Which Strains Recorded		
2	1,000	200	3,000
3	3,000	4,000	5,000
4	3,000	4,000	5,000
5	2,500	—	—

4-ft intervals. These pavements had been under normal traffic for approximately 9 years. There were very slight and localized systems of distress which indicated that their design was adequate for the traffic carried before the test. The test pavements were divided into four separate sections. Each section was subjected to repetitions of a single load. The four loads were 18-kip single axle, 22.4-kip single axle, 32-kip tandem axle, and 44.8-kip tandem axle.

Description of the Project. — Concrete Pavements. — The concrete in these slabs had an average compressive strength of 6,825 psi, an average modulus of rupture of 785 psi. The design cross-section thickness was closely approximated in construction according to field measurements. The static modulus of elasticity varied from 4,200,000 to 5,003,000. A value of 5,000,000 was used for all strain-to-stress conversion. The sonic or dynamic modulus averaged 5,700,000 for air-dried conditions and about 5,900,000 for wet specimens.

Subgrade Conditions. — The subgrade classifications and variation for the four test sections are given in Table 5.

Program of Strain Measurements. — Strains were measured for a variety of loads including the standard cases of interior loading, edge loading and corner loading. The results of the free edge load and the corner load conditions are primarily dealt with herein. Figure 14 shows these loadings with reference to the slab. Various studies were made on these test pavements. Those discussed in this comparison are load-stress relationships, speed-stress relationships, variation of stress with temperature differentials with the slab and variation of stress with subgrade support conditions.

Strains were measured with SR-4, type A9 (6-in. length electrical resistance) strain gages. All strain values were recorded with a direct-writing oscillograph. The strain gages were cemented into place on the slab surface and sealed with appropriate waterproof protection. Conversion of strain to stress was made using the appropriate elastic equations given in Report 5, Appendix E (2).

Pickett's Mathematical Studies

Pickett noted that several of the theoretical and empirical formulas developed for corner stresses in concrete pavement had poor boundary conditions. For example, the

TABLE 5

SUBGRADE CONDITIONS—MARYLAND ROAD TEST

Load No.	Max. Axle Loading (lb)	HRB Classification Group[a]				
		A-1	A-2-4	A-4	A-6	A-7-6
1	18,000 (single)	27	2	4	56	11
2	22,400 (single)	25	6	4	54	11
3	32,000 (tandem)	0	0	14	68	18
4	44,800 (tandem)	0	0	14	65	21

[a]Percent of total number of slabs in each lane supported by indicated soil.

Note: In general, the ratings of soils within these groups as a subgrade material are: (1) excellent for A-1; (2) good to fair for A-2-4; (3) fair to poor for A-4; and (4) poor for A-6 and A-7-6.

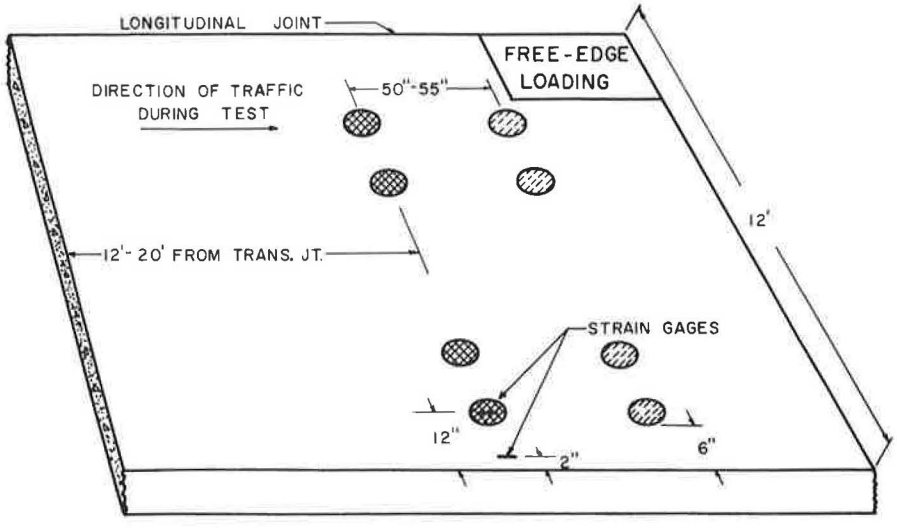

POSITION OF WHEELS AND LOCATION OF STRAIN GAGES FOR MEASUREMENT OF CRITICAL STRAINS FOR FREE-EDGE LOADING

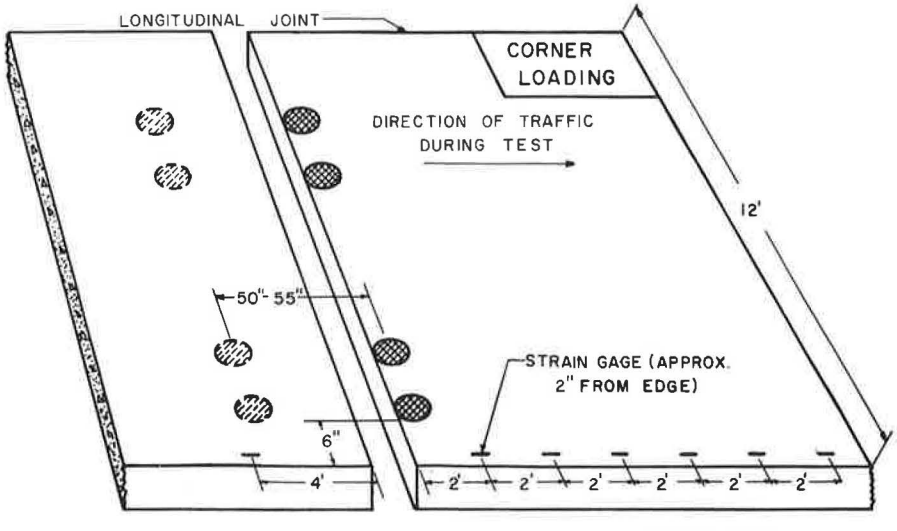

POSITION OF WHEELS AND LOCATION OF STRAIN GAGES FOR MEASUREMENT OF CRITICAL STRAINS FOR CORNER LOADING

Figure 14. Wheel positions for critical edge and corner strains.

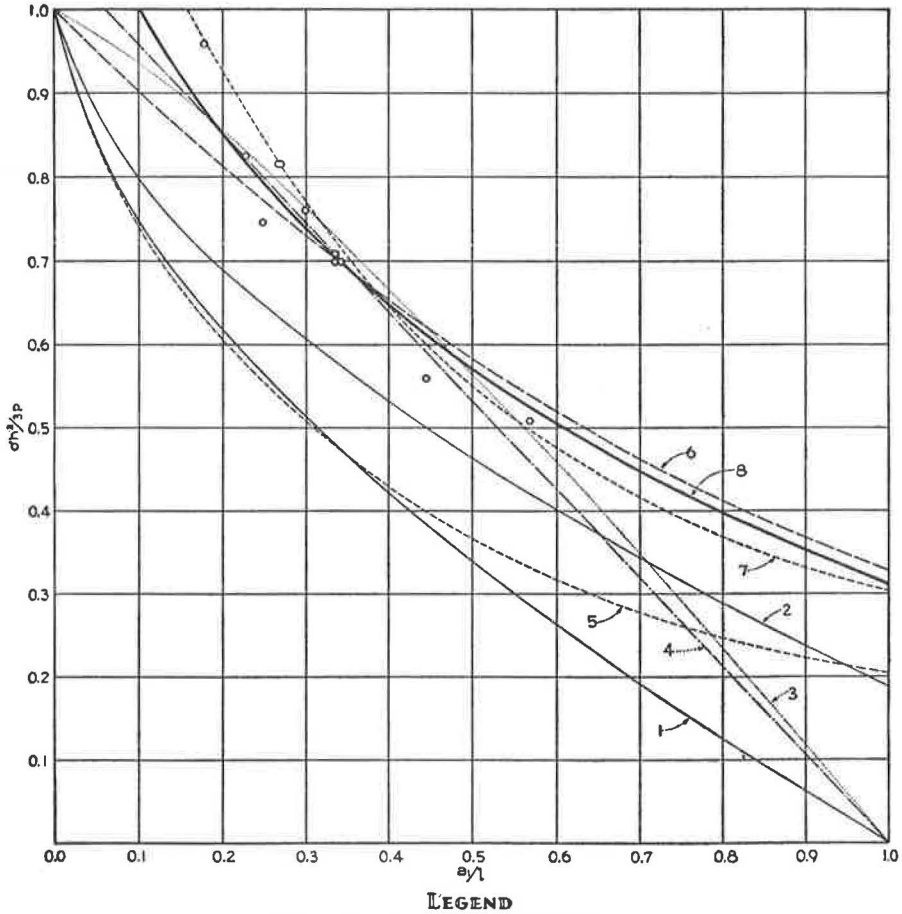

LEGEND

Curve 1 (Westergaard)	$\frac{dh^2}{3P} = 1-\left(\frac{a_1}{l}\right)^{0.6}$	Curve 5, Theoretical ———	Full subgrade support
Curve 2 (Bradbury)	$\frac{dh^2}{3P} = 1-\left(\frac{a_1}{\sqrt{2}l}\right)^{0.6}$	Curve 6, Theoretical ———	Partial subgrade support
Curve 3 (Kelley)	$\frac{dh^2}{3P} = 1-\left(\frac{a_1}{l}\right)^{1.2}$	Curve 7, Theoretical ———	50% increase over Curve 5
Curve 4 (Spangler)	$\frac{dh^2}{3P} = \frac{3.2}{3}\left[1-\frac{a_1}{l}\right]$	Curve 8, Semi-empirical ———	$\frac{dh^2}{3P} = 1.4\left[1-\frac{\sqrt{2}a_1}{1.1+\frac{0.185a_1}{l}}\right]$

° Plotted points represent experimental data furnished by the Public Roads Administration

Figure 15. Comparison of theory with existing stress equations.

Westergaard, Kelley, and Spangler equations all indicate stress to be zero when the ratio of the radius of the loaded area to the radius of relative stiffness equal 1.0 (Fig. 15). Because of these observations, Pickett has worked toward the development of a formula which has the shape and characteristics of the Westergaard equation, but which has more rational boundary conditions.

COMPARISON OF THEORETICAL AND OBSERVED STRESSES FOR CORNER LOAD CONDITIONS

Many of the concrete pavement design equations used in the past 30 years have been corner equations. Thus, it is interesting to compare all available information with the Road Test experimental results for the case of corner loads.

BPR Arlington Tests

Effect of Modulus of Elasticity on Indicated Stresses. — Figure 16 shows in solid lines the comparison of indicated and theoretical stresses in the 6-, 7-, 8-, and 9-in. slabs. The stresses were obtained by using an average value of E determined for the corner load conditions. Table 6 indicates that this value of E is considerably lower than E determined from the other two load conditions. The authors of the BPR report therefore calculated the values shown in dashed lines by using the average E for interior and edge loading. In their opinion, the theoretical (Westergaard) and observed stresses agree closely for the 6- and 8-in. slabs because these slabs were tested when warped

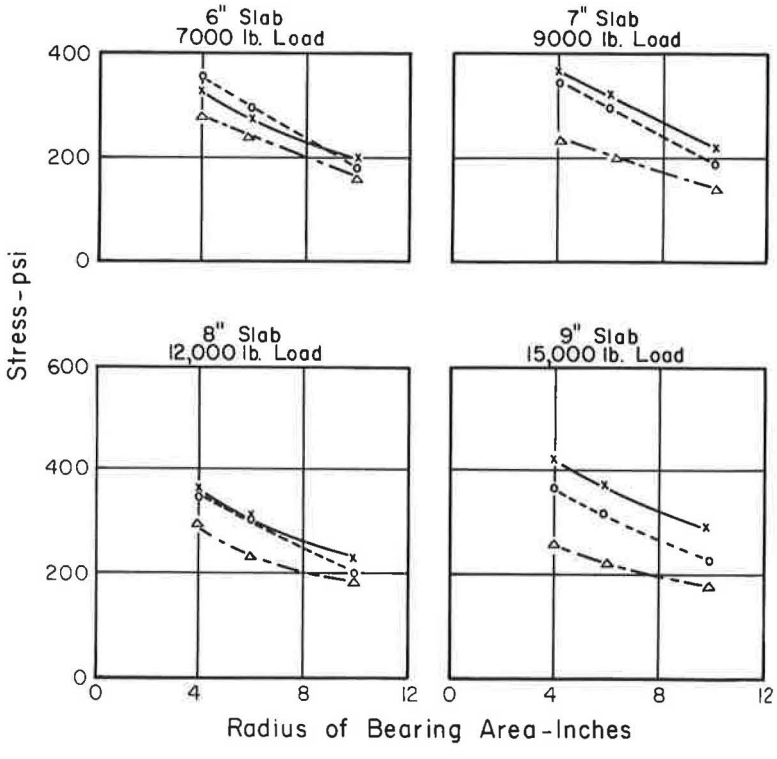

Figure 16. Comparison of theoretical and observed stresses for corner load.

TABLE 6

VALUES FOR VARIOUS COEFFICIENTS, WESTERGAARD EQUATIONS, DETERMINED FROM MEASURED DEFLECTIONS, BPR TESTS[a]

Load Position	Testing Time	Slab Thickness (in.)	l (in.)	k (pci)	K (psi)	D (psi)	E (psi)
Corner	Late summer	6	26	143	3,708	96,400	3,540,000
	Winter	7	28	161	4,515	126,400	3,390,000
	Winter	8	30	227	6,825	204,700	4,220,000
	Late fall	9	33	168	5,535	182,600	3,200,000
Interior	Late summer	6	25	195	4,880	122,000	4,140,000
	Winter	7	29	238	6,895	200,000	5,750,000
	Summer	7	28	222	6,230	174,400	4,670,000
	Winter	8	31	260	8,065	250,000	5,500,000
	Late fall	9	36	203	7,315	263,200	5,490,000
	Summer	9	33	220	7,290	240,500	4,210,000
Edge	Late summer	6	26	171	4,440	115,400	4,235,000
	Winter	7	29	212	6,145	178,200	5,125,000
	Winter	8	30	279	8,365	251,000	5,175,000
	Late fall	9	34	243	8,260	280,800	5,220,000

[a]Source: Public Roads, 23:8, p. 187.

downward. Observed stresses for the 7- and 9-in. slabs were higher than theory indicates because they were tested while warped upward. Additional tests on the 7- and 9-in. slabs while warped down seem to verify these observations. The following conclusions were drawn:

1. Values of E calculated for corner leading conditions are unrealistic.
2. If the conditions are such that the corner is receiving full subgrade support, values of critical stress for corner loading (Case 1) computed from the Westergaard equation can be used with confidence. When full support does not exist the computed stresses will be too low.

Variation of Critical Stresses with Slab Curling or Warping. — The authors compared critical or maximum load stresses observed for three positions of the slab: (a) corners warped up, (b) flat, and (c) corners warped down. Table 7 gives a compilation of these values with the comparative values of maximum stress observed at the Road Test (formulas were used to interpolate for the correct load and slab thickness).

Figure 17 shows the stress-slab thickness comparisons for the Arlington and Road Test experiments as well as for several stress equations. The Road Test stresses are considerably smaller than the BPR stresses or the theoretical stresses. The Road Test stresses are those due to dynamic (transient) loads (load time $^1/_{12}$ sec), whereas the BPR stresses are those under a static load (load time 5 min). The Road Test stresses were also measured at a corner with a doweled joint, whereas the BPR slabs had free joints and edges. Based on a comparison of other strain studies at the Road Test it appears likely that one-fourth to one-third of the load is transferred to the adjacent slab, thus reducing the induced strains and, thus, stresses in the study by 25 to 33 percent.

Directions of Maximum Principal Stresses. — In connection with the main studies, the BPR made some supplementary studies to indicate the direction and magnitude of the principal stresses induced by corner loads (Figs. 18 and 19). An 8-in. uniform

TABLE 7

COMPARISON OF CRITICAL STRESSES
BPR ARLINGTON TEST AND AASHO ROAD TEST

Wheel Load	Slab Thick (in.)	Arlington BPR			Theoretical Westergaard Case 1	AASHO Road Test	
		Warped Up	Flat	Warped Down		Warped Up[a]	Warped Down[b]
5k	6	288	274	228	200	91	46
7k	7	325	308	253	218	95	48
10k	9	290	277	220	210	92	47

[a]Night. [b]Day.

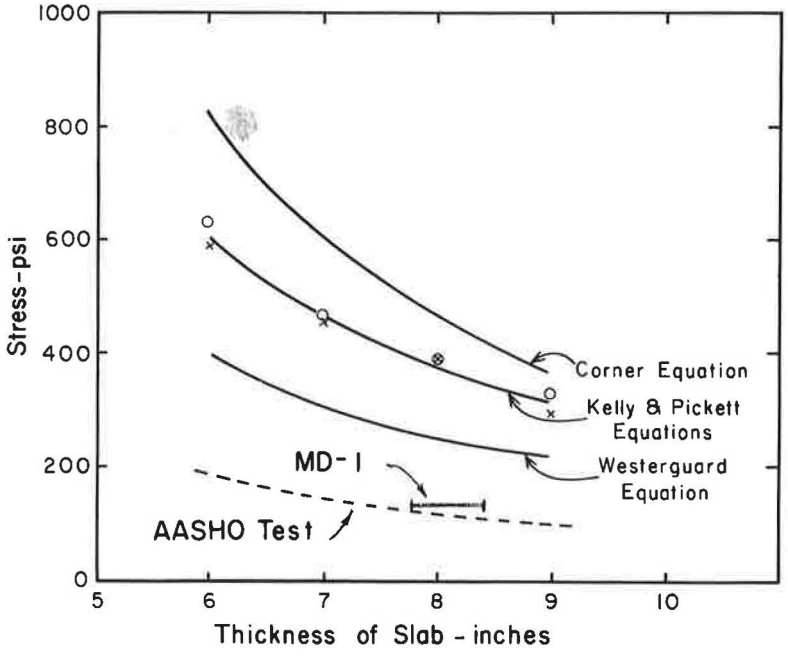

NOTE:

1. Plotted points represent data from B.P.R. Arlington Tests with 10,000 pound load, 12 inch diameter bearing area.

2. Dotted curve represents observed stresses from AASHO Road Test. Fitted Equation: $\sigma_c = \frac{385 L_w}{h^{1.7}}$

Figure 17. Comparison of observed stresses with four stress equations.

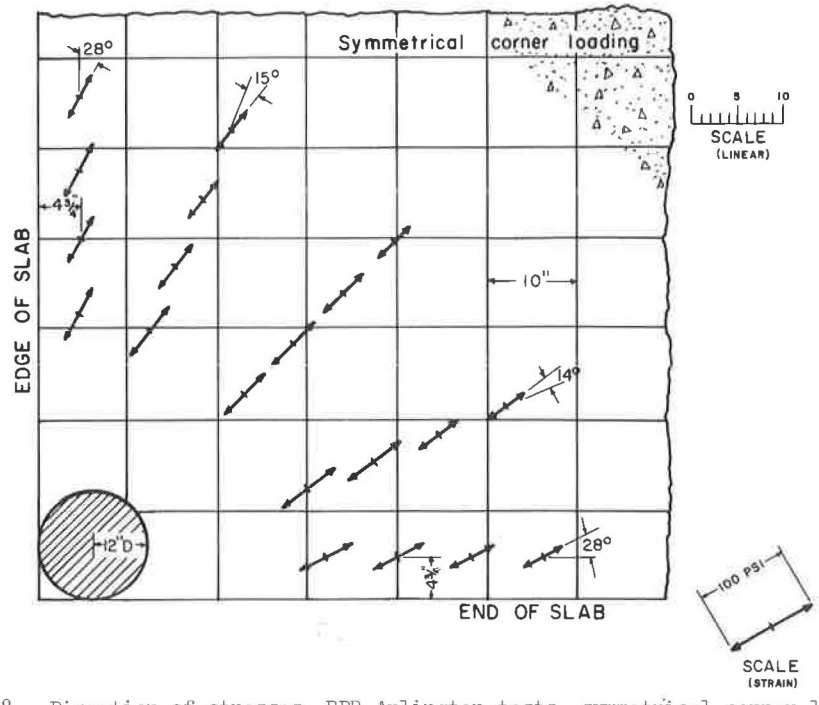

Figure 18. Direction of stresses, BPR Arlington tests, symmetrical corner loading.

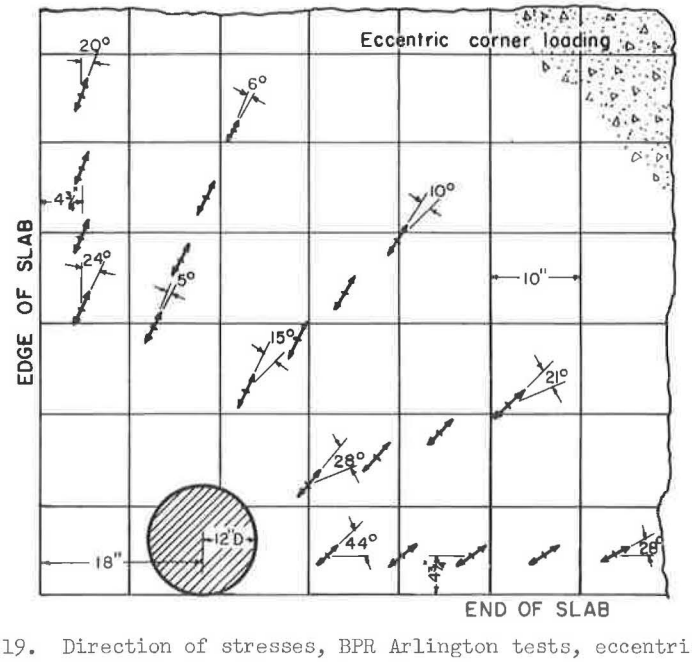

Figure 19. Direction of stresses, BPR Arlington tests, eccentric corner loading.

thickness slab and a 9-6-9-in. slab were compared with a symmetrical corner load and an eccentric corner load (Fig. 19). Moving the load from the corner toward the centerline 18 in. caused a shift in the direction of maximum stresses. The shifts were counter-clockwise angular displacements of 7 to 14 degrees.

Kelley's Empirical Equation. — To summarize their work on corner stresses the authors of the BPR report indicate that the Westergaard equation for Case 1 (Eq. 4) gives an accurate indication of maximum load stress when the pavement corner is in full contact with the subgrade. In the BPR investigation this condition was attained only when the corner was warped downward. If Eq. 4 is used for computing load stress, the condition of corner warping due to temperature would be such as to create a moderate compressive stress in the upper surface of the slab in the region where the load would create the maximum tensile stress. Thus the combined stress would be slightly lower than the load stress.

For other cases when the slab corner is not in complete bearing on the subgrade due to upward warping, Eq. 4 will give load stress values somewhat lower than those which are actually developed. For this condition the Arlington experiments indicate an empirical equation which gives computed values which are more nearly in accord with those observed. This equation was reported by Kelley in 1939 (9).

$$\sigma_c = \frac{3\,P}{h^2}\left[1 - \left(\frac{a_1}{\ell}\right)^{1.2}\right] \qquad (23)$$

in which

σ_c = maximum tensile stress, in psi;
P = load, in lb;
h = thickness of concrete slab, in in.;
a_1 = the distance, in in. from the corner of the slab to the center of the area of load application; it is taken as $a\sqrt{2}$ where a is the radius of a circle equal in area to the loaded area;
$\ell = \frac{Eh^3}{12\,(1 - \mu^2)\,k}$ = radius of relative stiffness;
E = Young's modulus for the concrete, in psi;
k = subgrade modulus, in psi/in.; and
μ = Poisson's ratio for the concrete.

To summarize, as a general rule the most critical condition for the corner loading is at night when the corner tends to warp upward; the subgrade support is least effective at that time. Any warping stress in the corner is also additive to the load stress.

Iowa State College Tests

New Hypothesis for Stress Distribution in Corner Region. — The Westergaard corner equation and the Older corner equation both imply the same assumption of uniform distribution of the maximum tensile stresses along a line normal to the corner bisector. Observations of stress and observation of structural corner breaks both in the laboratory and the field, led Spangler to the hypothesis that the locus of maximum moment produced in a concrete pavement slab by a corner load is curved line which bends towards the corner as it approaches the edge of the slab. It appears that the locus may lie anywhere between a straight line normal to the bisector (Westergaard assumption) and a circular curve tangent to that bisector having the corner as its center. Under this hypothesis the maximum stress will occur when the locus is a circular curve inasmuch as this is the shorter of the two limiting sections.

Figure 20, from the Spangler report, shows these limiting conditions along with a typical corner break.

Stress Direction and Magnitude. — Figures 21 and 22 indicate the direction and magnitude of principal stresses in slab 4 (6-in. thickness) under a 5,000-lb static load.

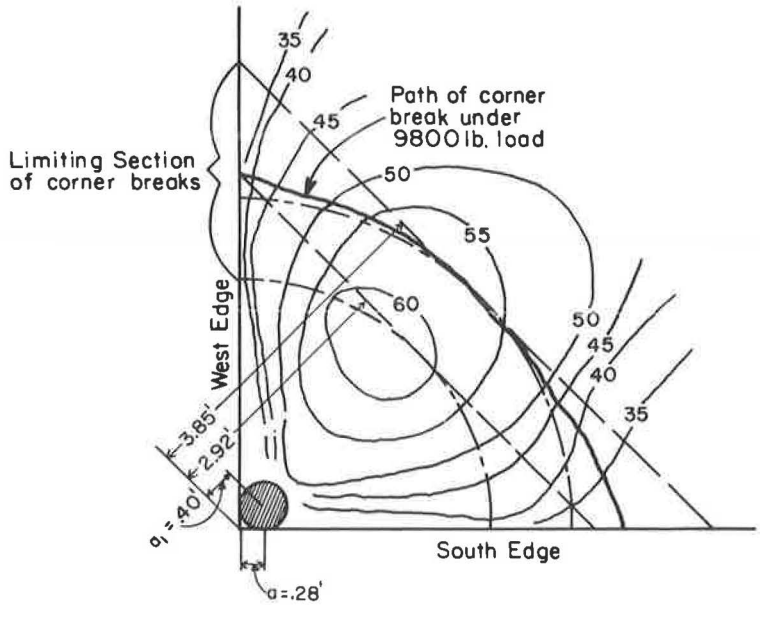

Figure 20. Stress contours for Iowa State College tests.

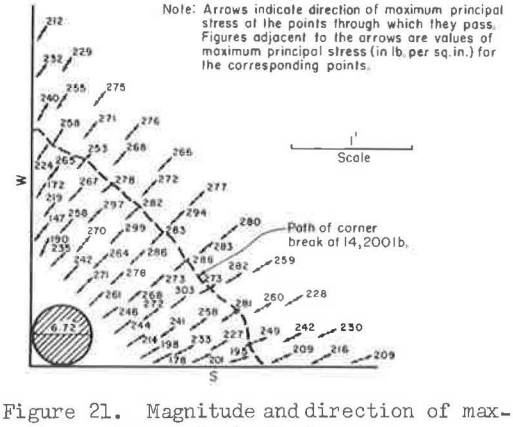

Figure 21. Magnitude and direction of maximum principal stresses.

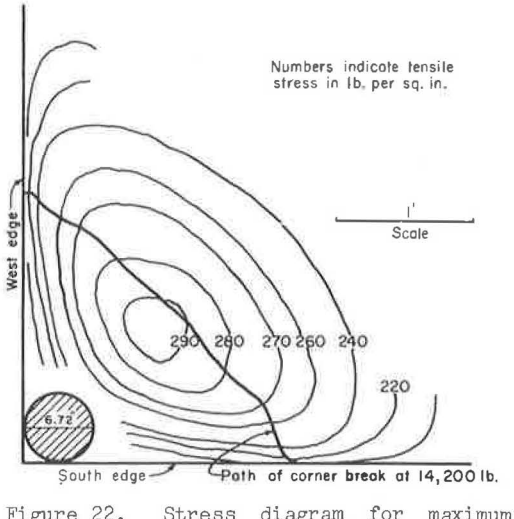

Figure 22. Stress diagram for maximum principal stress Iowa State College tests.

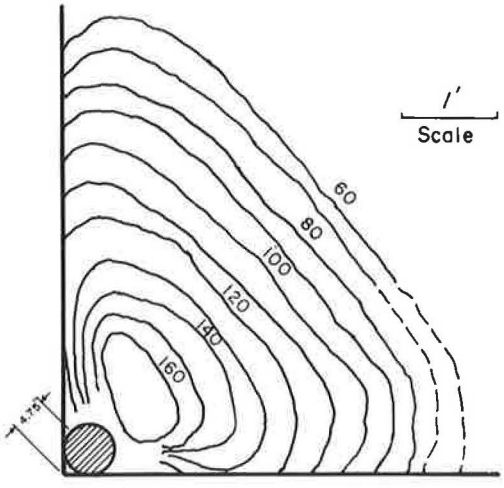

(a) Circular shape tangent to edges.

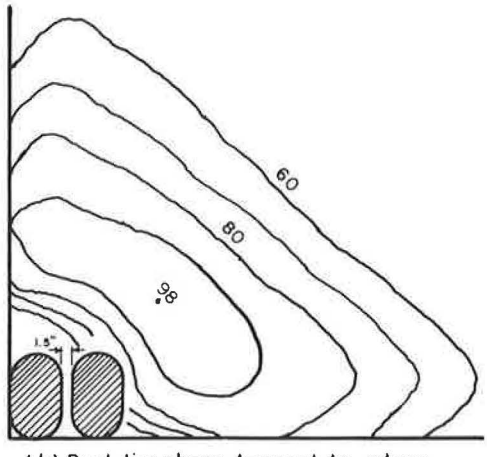

(b) Dual tire shape tangent to edges.

Note: Contours connect points of equal intensity of principal tensile stress. Values given are in lb. per sq. in.

Figure 23. Stress contours for slab 3, Iowa State tests.

These values were obtained by averaging readings from three separate loadings of the slab.

Slab 3 (6-in. thickness) was a smaller experiment than slab 4. Figure 23 shows the approximate principal stress contours observed on this slab for a circular and an elliptical load. As in slab 4, there is a considerable area over which the stress in slab 3 does not vary greatly. Although the slabs were of the same nominal thickness and approximately the same size, the maximum stress in slab 3 was only about 50 percent of that in slab 4. Spangler makes the following observations: "This is probably due to the fact that the subgrade under Slab 3 was stiffer than that under Slab 4 and that the modulus of elasticity of the concrete in Slab 3 was less than of Slab 4. It is difficult, however, to account for such a divergence in stress in this way since published analyses of stresses indicate that large variations in either or both of these coefficients cause relatively small variations in stress."

Iowa Study Conclusions

Table 8 compares the observed stresses in these studies with existing stress equations. It was concluded that in these studies observed stresses were in general agreement with the equation proposed by Kelley. The Kelley equation actually gives calculated stresses that closely agree with the observed stresses only for slab 2.

The Westergaard equation shows excellent agreement with the observed stresses for both slabs 4 and 5 and does not show too large a variation for slab 2. Since these slabs were constructed and tested in a closely controlled environment, to eliminate temperature and moisture curling, it would appear that the observed stresses should check the Westergaard equation more closely than the Kelley equation.

Maryland Road Test—Corner Load

The corner load-strain measurements at the Maryland and AASHO Road Tests were not as complete as the edge measurements. For that reason these comparisons will not be extensive. Comparisons will be made of load vs stress relationships and effects of corner warping (temperature differential).

These comparisons are further complicated by the nonuniform slab thickness of the Maryland pavements. In an effort to overcome this difficulty, results for several thicknesses from the AASHO tests have been compared with the Maryland data.

In the analysis of data from the Maryland test, static modulus of elasticity was used in the conversion of strains to observed stresses, whereas in the AASHO results

TABLE 8

COMPARISON OF STRESS EQUATIONS AND OBSERVED STRESSES—CORNER LOADING
(Iowa State College Tests)

Stress	Slab 2	Slab 4	Slab 5	Avg.
Westergaard Eq.	170	260*	255*	228*
Kelley Eq.	215*	350	415	326
Corner Eq.	250	410	470	376
Observed	230	285	215	243

*Indicates equation giving closest prediction for that slab.

tion existed with the slab warped down (day measurements). At the AASHO test after 26 series of such experiments, it was concluded from regression analyses that the relationship was a straight line within the limits of significant statistical error. There was some indication, however, that the relationship might be curvilinear for weaker subgrades.

Figure 24 shows that the indicated stresses from the MD-1 test approximate the stresses in a 7-in. slab at the AASHO test for conditions of upward warping. For conditions of downward warping, the MD-1, 9-7-9-in. slab acted much like an 8-in. slab at the AASHO test. This last comparison is considered to be the more valid since strain measurements of a slab on two different reasonably hot afternoons will agree without significant variation; whereas strains measured on two different mornings may vary considerably depending on moisture and temperature. Therefore, the general condition of downward warping is more stable than upward warping.

Effect of Corner Warping.—Additional complications arise with this comparison since quantitative information is not available about temperature differentials which existed at the time strains were measured. (The report merely indicates slabs warped up, flat or warped down.) The amount of warping, or more specifically the exact temperature differential of top minus bottom of the slab is very important in absolute strain existing. It can generally be concluded that the apparent effect of warping or curling was much the same for the Maryland and the AASHO Road Tests.

dynamic E was used. It seems that a common type of E must be used if comparisons are to be valid. In the following work dynamic E has been used since the loads involved were dynamic or moving loads.

Load vs Stress.—Figure 24 shows a comparison of load-stress relationships at the two road tests. The MD-1 report indicates that a curvalinear relationship was found for slabs warped upward (early morning); whereas a straight-line rela-

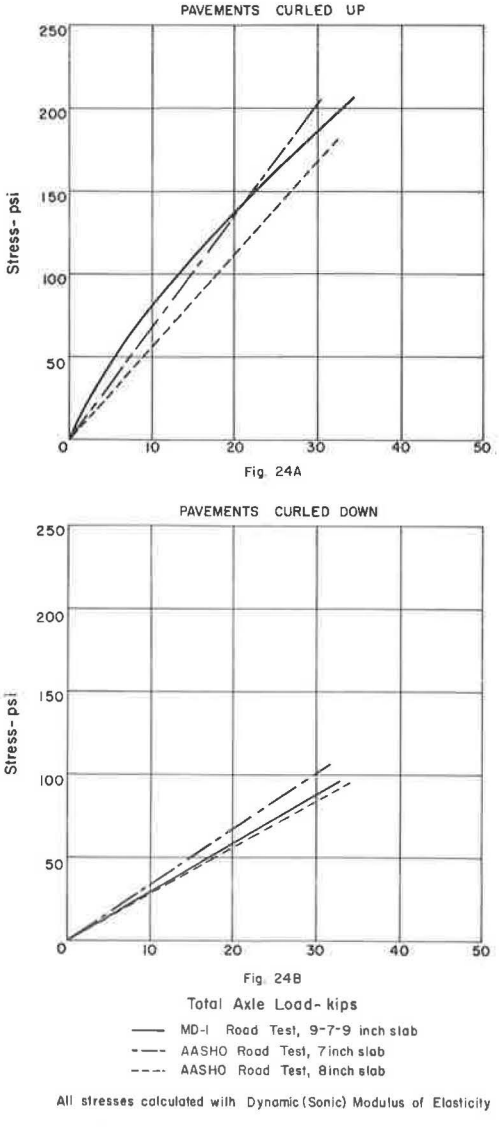

Figure 24. Load stress comparisons and effect of corner warping on stresses.

COMPARISON OF THEORETICAL AND OBSERVED STRESSES FOR EDGE LOADING

Edge loading was one of the three cases originally investigated by Westergaard. Study of these edge stresses has become more important with the advent of load transfer devices to help limit corner stresses. The use of longer joint spacing on reinforced concrete slabs and finally the development of continuously-reinforced concrete pavements have increased the need to study edge stresses. The largest strain experiment at the AASHO Road Test was measurement of edge strains. The most important edge strain experiments reported prior to the AASHO Test include the Bureau of Public Roads' Arlington Tests (4) and the Maryland Road Test (12).

In the AASHO tests, stresses under edge loads were generally higher than the stresses under corner loads. Figures 7 and 9 show some of the results of these tests. In all cases the maximum edge stresses occurred directly opposite the load. For tandem axles the maximum occurred opposite one of the pair of axles, usually the rear axle.

BPR Arlington Tests

The conditions of the BPR test and the AASHO Road Test have previously been discussed. It was necessary to adjust the AASHO results to conditions approximating the BPR test to compare the results. The following adjustments in the equation were made using experimental results from the Road Test:

1. Stresses will be 22 percent higher at creep speed, which is as nearly static as was tested.
2. Stresses will increase 24 percent due to change in placement of loaded wheels to approximate BPR placement.

The resulting equation for stresses at the Road Test which can be compared to the BPR tests is

$$\sigma_e = \frac{211\ L_1}{10^{0.0031T}\ D^{1.28}} \tag{24}$$

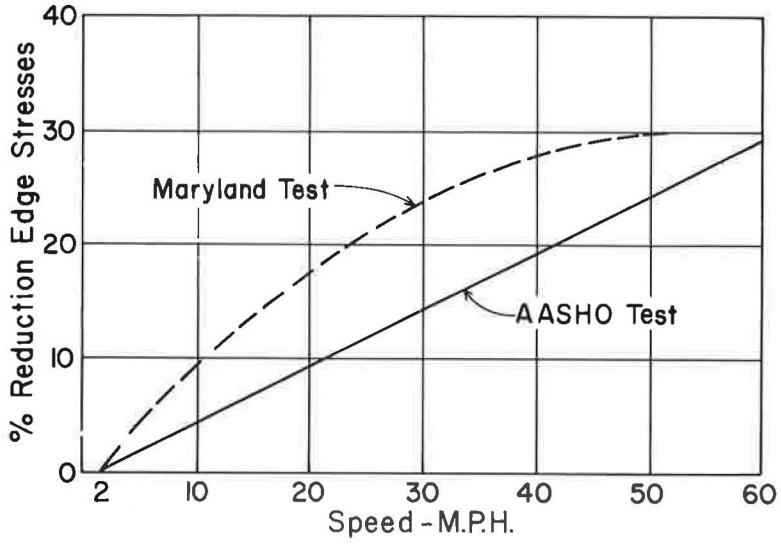

Figure 25. Effect of vehicle speed on pavement edge stresses.

or

$$\sigma_e = \frac{422\ P}{10^{0.0031T}\ D^{1.28}} \tag{25}$$

in which L is the axle load and P is a half axle load or wheel load. Other terms have previously been defined.

A static modulus has been used to convert the BPR strains because the load was static of 5-min duration. A dynamic modulus is assumed to apply for the AASHO Road Test since the load was always moving.

Stress Variation with Load. —To compare load study result, T is set equal to zero since no mention of warping conditions was made in this regard (4, Fig. 26). The results of this comparison are shown in Figure 26 for a 7-in. and 9-in. uniform thickness concrete slab. The load vs stress relationships are linear in all cases and the results for a given thickness very nearly agree. This indicates that the effect on stress of increasing the load might be expected to be the same on two pavements if the major physical variables such as temperature differential, load placement, and slab thickness are equal for the two pavements.

Stress Variation with Slab Thickness. —In the BPR report the effect of slab thickness was illustrated (4, Fig. 43). These data are shown in Figure 27. The basic information presented is for a study with pavement edges curled up. A similar curve for flat slabs has been developed by adjusting BPR data to a common load of 10,000 lb. Road Test data for both the curled up and flat positions are shown. A comparison of these curves indicates that the effect of curling was probably more severe on the BPR pavements than on the Road Test. This is to be expected because the BPR slabs had

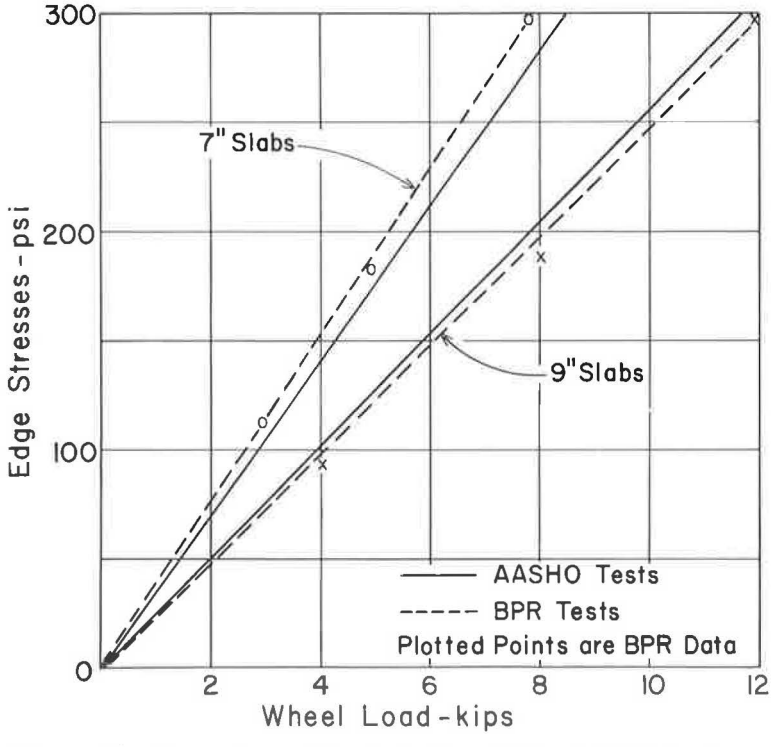

Figure 26. Comparison of load studies, BPR and AASHO tests.

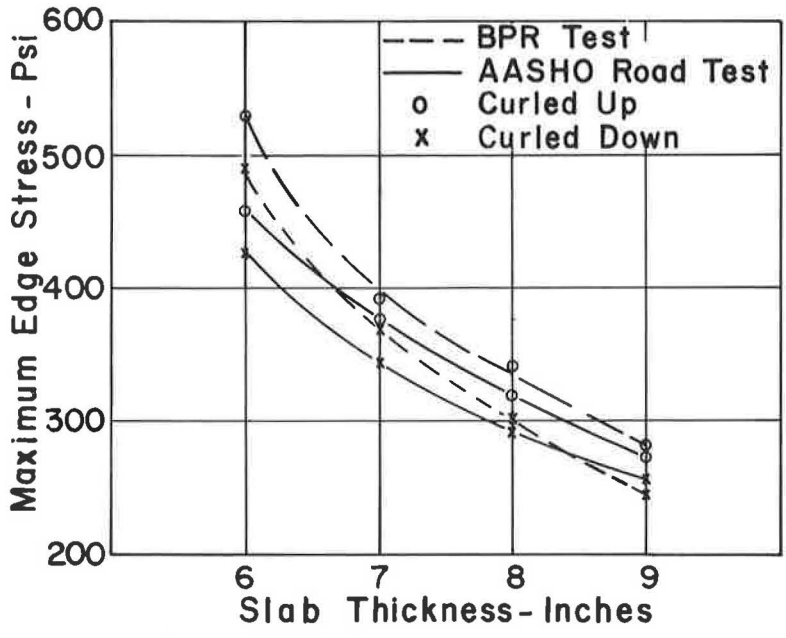

Figure 27. Effect of slab thickness, BPR and AASHO.

no adjacent slab giving restraint, whereas the Road Tests slabs were doweled to adjacent slabs. Further examination shows a variation in the shape of the curves which results in a cross at 8 in., thus explaining why Figure 26 shows BPR stresses higher on 7-in. slabs, but lower on 9-in. slabs. Figure 28, a plot of Westergaard's equation (Eq. 8) for the BPR physical conditions, agrees almost perfectly with the BPR "flat condition" data.

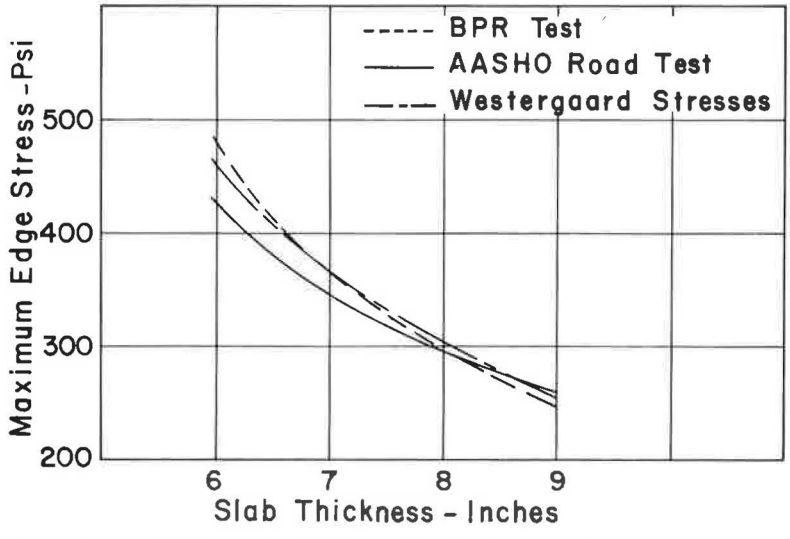

Figure 28. Comparison of BPR and AASHO with Westergaard equations for curled down pavements.

Maryland Road Test

To compare results, certain adjustments must be made in the AASHO stress equation and the Maryland data. Where reliable data were developed as part of the tests, the following changes were required:

1. The standard placement for the Maryland test was 3 to 4 in. nearer the edge than the AASHO Test. (For the AASHO Test the centroid of the loaded area was located 20 inches from the pavement edge.) Using published data (12, Fig. 13), Maryland results were adjusted to the AASHO placement.
2. In some cases the AASHO equation was adjusted to creep speed.
3. The Maryland tests involved normal dynamic vehicle loads.

At the AASHO Road Test the decision was made to use dynamic modulus of elasticity (E_d) with dynamic loads. For comparisons, the Maryland report gives results of load studies for pavement "warped or curled" up. To compare these results with the AASHO data, T (Eqs. 14 and 15) was taken as 7 degrees, a condition of moderate upward curl (-10° was the maximum negative temperature differential T observed at the Road Test). Figure 29 compares the load vs stress curves for the Maryland and AASHO Road Tests.

For single-axle loads the stresses on the 9-7-9-in. Maryland pavements were approximately equal to the stresses in a 9-in. uniform thickness pavement at the AASHO test. This indicates effective reduction of edge stresses by use of edge thickening.

For tandem-axle loads the stresses in a 8-in. AASHO Road Test slab closely approximate the stresses observed for the Maryland slabs. This indicates an averaging effect of the 9- and 7-in. portions because the stresses, although smaller than might be expected in a 7-in. thick slab, are not as small as they probably would have been for a 9-in. uniform thickness slab. The difference in the action of the 9-7-9-in. slab under the two types of load may be due to the broader stress patterns of the tandem loads. In other words, the tandem axles spread the load in such a way that a larger percentage of the 7-in. portion of the Maryland slabs comes into action. The apparent difference may be only experimental error in testing conditions though it is not likely since averages are used in the comparisons and no major known biasing effect is involved.

The load vs stress studies in the Maryland test indicate non-linear action (Figs. 29 and 30). The AASHO results show a linear effect. It is important to note that during the AASHO Test several individual studies indicated non-linear action. For the total picture, a linear equation always fits the data better than a non-linear one.

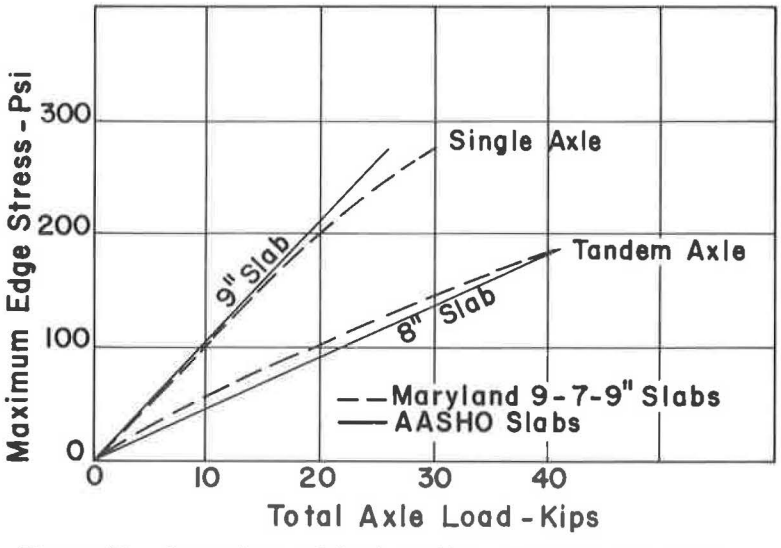

Figure 29. Comparison of load studies, Maryland and AASHO.

It was the conclusion at the AASHO Test that the load effect was linear, and it is believed that this holds true in general. It appears, however, that unexplained interaction effects may result in non-linear behavior for any given case study. Inasmuch as the Maryland tests were primarily case studies, this could explain the non-linear effect.

Variation of Stresses with Curling. — Curling, the warping of concrete pavements due to vertical internal temperature differential in the slab, affects the stresses in a concrete slab. A pavement which is curled upward will ordinarily exhibit higher compression stresses in the top than one which is curled downward. This was found to be true for both the Maryland and the AASHO Road Tests.

Figure 30 compares stresses in the AASHO and Maryland test pavements curled upward and downward. For both the single- and tandem-axle loads, the Maryland pavements indicate a greater reduction in stress from curled up to curled down condition than do the AASHO pavements. The stresses in the Maryland pavements were 28 percent smaller for the curled down condition than for the curled up condition, whereas the stresses for the AASHO pavements were 19 percent smaller for the down than for the up condition.

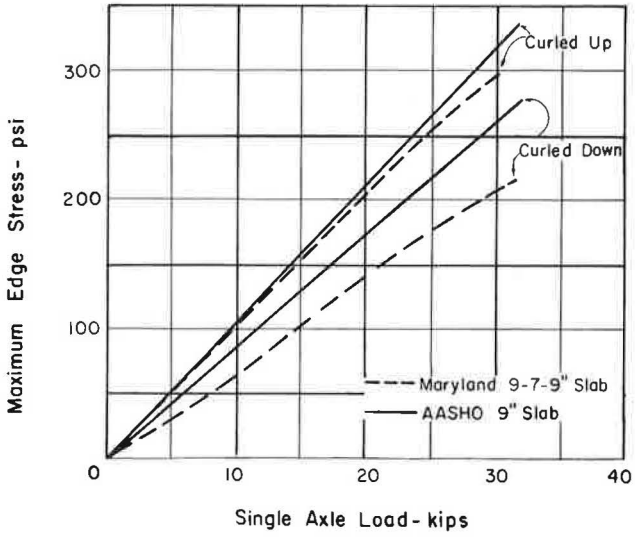

Fig. 30A

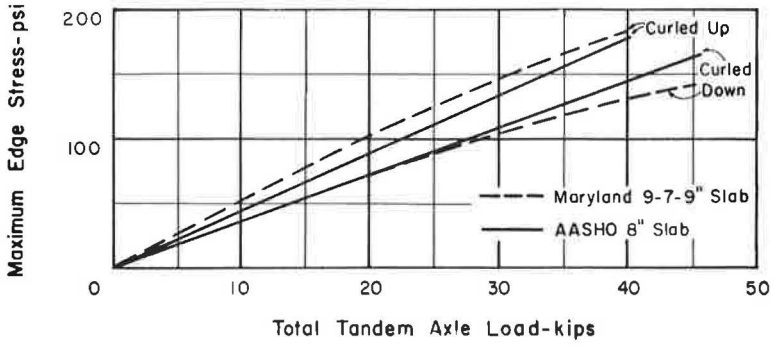

Fig. 30B

Figure 30. Effect of pavement curling, Maryland and AASHO.

This situation is hard to explain because during a 2-yr period on the AASHO Test only 1 percent of the observations of pavement temperature differential shows T greater than +20°. This was, therefore, taken as the maximum downward curl condition and used in these comparisons. The minimum differential was -10° for the up condition. Either the maximum temperature differential was greater in the Maryland test for the days involved or other conditions affecting curling warping (moisture, humidity, etc.) affected the results.

Summary of Edge Stress Comparisons

1. For equivalent conditions of load placement, vehicle speed, temperature differential within the slab, and physical constants, slab stresses vary in direct linear proportion to the load.
2. The load effects in the BPR test and the AASHO tests were equivalent within the limits of experimental error.
3. The edge stresses observed for the 9-7-9-in. slabs on the Maryland test were equivalent to the stresses in a 9-in. AASHO slab for single axles and an 8-in. AASHO slab for the tandem axles.
4. The variation of stress with slab thickness was regular for both the BPR and the AASHO tests. The BPR data for the flat or curled down condition is closely approximated by the original Westergaard equation. The Road Test results, however, show a smaller effect of thickness.
5. The general effect of pavement curling was observed to be the same in all tests. However, the effect of curl on stresses reported for the Maryland test was greater than any observed at the AASHO Road Test.

SUMMARY OF NEEDED RESEARCH

As a result of these dynamic studies, it appears that there is a need to study the effect of physical constants with relation to dynamic loads. It is believed that such a study would ultimately lead to a design equation relating all these factors in a manner similar to that proposed in the AASHO Rigid Pavement Design Guide, May 1962.

It would be desirable to study the effect of dynamic loads as related to modulus of elasticity, modulus of subgrade support, and strength of the concrete. There is sufficient proof available from the AASHO Road Test to indicate that such a study is both physically and economically feasible by employing a vibrating loader similar to that introduced at the Road Test.

Additional studies should be made on numerous factors including: (a) various types of load transfer devices, and (b) various types of supporting media including granular materials and various stabilized materials.

A large area of research is the combination of load-stresses with warping stresses in order to investigate the ultimate failure stresses in the pavement.

SUMMARY OF FINDINGS

Corner Load Stress Comparisons

1. The stresses predicted by the Westergaard equation, the corner load equation, or the Pickett equation are considerably higher than those observed at the AASHO Road Test. This is probably because (a) the effect of dynamic loads is not as great as a sustained static load of the same magnitude, and (b) the Road Test slabs were doweled to adjacent slabs and were not as free to deflect as theoretical equations predict.
2. The stresses observed for the Maryland test 9-7-9-in. slabs approximated those of 7- and 8-in. slabs at the AASHO Road Test in a curled up and curled down condition.
3. The directions of principal stresses are not symmetrical about the corner bisector for dual-tire loadings. The pattern is further altered if the slab joints are not free from restraint by other slabs.
4. The effect of slab warping or curling was observed to be much the same for the Maryland and AASHO Road Tests.

5. The load vs stress relationships at the Maryland and AASHO Road Tests were approximately equal and linear. There is some indication that slabs curled upward show non-linear variation of stress with load as the bottom support increases with increased load.

6. In future studies of pavement stresses a special effort should be made to obtain complete information concerning the physical factors affecting these stresses, including modulus of elasticity, modulus of subgrade support and concrete strength.

Edge Load Stress Comparisons

1. For equal load placement, vehicle speed, temperature differential within the slab, and physical constants, slab stresses vary in direct linear proportion to the load.

2. The load effects in the BPR tests and the AASHO tests were equivalent within the limits of experimental error.

3. Edge stresses observed for the 9-7-9-in. slabs on the Maryland test were equivalent to the stresses in a 9-in. AASHO slab for single axles and an 8-in. AASHO slab for tandem axles.

4. The variation of stress with slab thickness was regular for both the BPR and the AASHO tests. The BPR data for the flat or curled down condition is closely approximated by the original Westergaard equation. The AASHO Road Test results however show a smaller effect of thickness.

5. The general effect of pavement curling was observed to be the same in all tests. However, the effect of curl on stresses reported for the Maryland test was greater than any observed at the AASHO Road Test.

ACKNOWLEDGMENTS

This report was made possible through the work of the AASHO Road Test committees, staff and workers, particularly Frank Scrivner, Rigid Pavement Research Engineer. Appreciation is due to Bert Colly for assistance in the Road Test strain experiments and for his leadership in this field.

Recognition is also due to the Texas Highway Department personnel who participated in the preparation of this report, particularly Miss Patsy White. This work was done under the general supervision of T. S. Huff and M. D. Shelby, whose continued encouragement in the preparation of this report is appreciated.

REFERENCES

1. Carey, W. N., Jr., and Irick, P. E., "The Pavement Serviceability-Performance Concept." HRB Bull. 250, 40-58 (1960).
2. "The AASHO Road Test: Report 5—Pavement Research." HRB Special Report 61E, 352 pp. (1962).
3. "The AASHO Road Test: Report 2—Materials and Construction." HRB Special Report 61B, 173 pp. (1962).
4. Teller, L. W., and Sutherland, E. C., "The Structural Design of Concrete Pavements." Public Roads, 16:8, 9, and 10; 17:7 and 8; 23:8.
5. Spangler, M. G., "Stresses in the Corner Region of Concrete Pavements." Iowa Engg. Exp. Sta. Bull. 157 (1942).
6. Westergaard, H. M., "Stresses in Concrete Pavements Computed by Theoretical Analysis." Public Roads, 7:2 (April 1926).
7. Westergaard, H. M., "Analytical Tools for Judging Results of Structural Tests of Concrete Pavements." Public Roads, Vol. 14 (1933).
8. Westergaard, H. M., "New Formulas for Stresses in Concrete Pavement of Airfields." ASCE Proc. 73:5 (May 1947).
9. Kelley, E. F., "Application of the Results of Research to the Structural Design to Concrete Pavements." Public Roads, Vol. 20 (1939).
10. "Concrete Pavement Design." Portland Cement Association, Chicago (1951).
11. Pickett, Gerald, Raville, M. E., Janes, W. C., and McCormick, F. J., "Deflections, Moments and Reactive Pressures for Concrete Pavements." Kansas State College Bull. No. 65, Engg. Exp. Sta. (Oct. 15, 1951).

12. "Final Report on Road Test One-MD." HRB Special Report 4, 142 pp. (1952).
13. "Results of Modulus of Subgrade Reaction Determination at the AASHO Road Test Site by Means of Pavement Volumetric Displacement Tests." Corps of Engineers, U.S. Army, Ohio River Division Laboratories (April 1962).

Appendix A

ELASTIC CONSTANTS—AASHO ROAD TEST PAVEMENTS

TABLE 9

MODULUS OF SUBGRADE SUPPORT (k)

Outer wheelpath	107
Inner wheelpath	109
Average	108

TABLE 10

DYNAMIC TESTS ON 6- x 6- x 30-IN. BEAMS

Max. Aggregate Size (in.)	Age	Dynamic Modulus of Elasticity, E (10^6 psi)			Poisson's Ratio, μ		
		No. Tests	Mean, $\bar{X}$	Std. Dev., S	No. Tests	Mean, $\bar{X}$	Std. Dev., S
2½	8 mo	11	6.14	0.31	11	0.28	0.047
	1 yr	11	6.14	0.38	11	0.27	0.044
1½	8 mo	10	6.39	0.25	10	0.28	0.075
	1 yr	10	6.20	0.61	10	0.25	0.035

TABLE 11

STATIC AND DYNAMIC TESTS ON 6- x 12-IN. CYLINDERS

Max. Aggregate Size (in.)	Age	Static Modulus of Elasticity (10^6 psi)			Dynamic Modulus of Elasticity (10^6 psi)		
		No. Tests	Mean, $\bar{X}$	Std. Dev., S	No. Tests	Mean, $\bar{X}$	Std. Dev., S
2½	3 mo	10	4.57	0.80	—	—	—
	1 yr	11	5.15	0.57	10	6.25	0.33
1½	3 mo	9	4.61	0.68	—	—	—
	1 yr	11	5.25	0.40	10	5.87	0.74

TABLE 12

SUMMARY OF TEST RESULTS ON HARDENED CONCRETE
(Obtained from Data System 2230)

Max. Aggregate Size (in.)	Loop	Flexural Strength[1], 14 Days			Compressive Strength, 14 Days		
		No. Tests	Mean (psi)	Std. Dev. (psi)	No. Tests	Mean (psi)	Std. Dev. (psi)
2½	1	16	637	46	8	3,599	290
	2	20	648	37	9	3,603	281
	3	71	630	44	38	3,723	301
	4	96	651q	38	48	4,062	288
	5	96	629	28	48	4,196	388
	6	99	628	51	48	3,963	325
	All	398	636	45	199	3,966	376
1½	1	4	676	65	2	4,088	162
	2	39	668	44	19	4,046	295
	3	24	667	47	14	3,933	440
	All	67	668	46	35	4,004	352

[1] AASHO Designation: T97-57 (6- x 6- x 30-in. beams).

TABLE 13

SUMMARY OF STRENGTH TESTS
(Obtained from Data System 2231)

Max. Aggregate Size (in.)	Age	No. Tests	Flexural Strength (psi)	
			Mean	Std. Dev.
2½	3 days	11	510	23
	7 days	11	620	34
	21 days	11	660	51
	3 mo	11	770	66
	1 yr	11	790	61
	2 yr	11	787	66
1½	3 days	12	550	37
	7 days	12	630	35
	21 days	12	710	53
	3 mo	12	830	41
	1 yr	10	880	53
	2 yr	12	873	48

Appendix B

CHARACTERISTICS OF MATERIALS—RIGID PAVEMENT (AASHO Road Test)

TABLE 14

PORTLAND CEMENT CONCRETE

Item	Pavement Thickness	
	5 In. and Greater	2½ and 3½ In.
Design characteristics:		
Cement content[1], bags/cu yd	6.0	6.0
Water-cement ratio, gal/bag	4.8	4.9
Volume of sand, % total agg. vol.	32.1	34.1
Air content, %	3-6	3-6
Slump, in.	1½-2½	1½-2½
Maximum aggregate size[2], in.	2½	1½
Compressive strength, psi:		
14 days	4,000	4,000
1 year	5,600	6,000
Flexural strength, psi:		
14 days	640	670
1 year	790	880
Static modulus of elasticity (10^6 psi)	5.25	5.25
Dynamic modulus of elasticity (10^6 psi)	6.25	5.87

[1] Type I cement.
[2] Uncrushed natural gravel.

TABLE 15

SUBBASE MATERIALS

Item	Value
Aggregate gradation, % passing:	
1½-in. sieve	100
1-in. sieve	100
¾-in. sieve	96
½-in. sieve	90
No. 4 sieve	71
No. 40 sieve	25
No. 200 sieve	7
Plasticity index, minus No. 40 material	N.P.
Max. dry density, pcf	138
Field density, as percent compaction	102

Appendix C

LIST OF SYMBOLS

a = radius of area of load contact, in in.; the area is circular in case of corner and interior loads and semicircular for edge loads.
a_1 = the distance, in in. from the corner of the slab to the center of the area of load application—taken as $a\sqrt{2}$ where a is the radius of a circle equal in area to the loaded area.
b = radius of equivalent distribution of pressure at the bottom of the slab.
D_2 = nominal thickness of the concrete slabs.
E = modulus of elasticity of the concrete, in psi.
h = thickness of the concrete slab, in in.
k = subgrade modulus, in pci.
ℓ = radius of relative stiffness.
L_1 = nominal axle load of the test vehicle (a single axle or a tandem-axle set).
P = point load, in lb.
T = the temperature (° F) at a point ¼ in. below the top surface of the 6.5-in. slab minus the temperature at a point ½ in. above the bottom surface, determined at the time the strain was measured (the statistic T may be referred to occasionally as "the standard differential").
ϵ = estimated edge strain at the surface of the concrete slab.
μ = Poisson's ratio for concrete.

σ_c = maximum tensile stress, in psi, at the top of the slab, in a direction parallel to the bisector of the corner angle, due to a load applied at the corner.

σ_e = maximum tensile stress, in psi, at the bottom of the slab directly under the load at the edge, and in a direction parallel to the edge.

σ_i = maximum tensile stress, in psi, at the bottom of the slab directly under the load, when the load is applied at a point in the interior of the slab at a considerable distance from the edges.

σ_{cv} = maximum load stress, in psi, as determined in Loop 1 for corner load.

σ_{es} = predicted stress under single-axle load.

σ_{et} = predicted stress under tandem-axle load.

σ_{ev} = the critical load stress, in psi, as determined under a vibratory load on the no-traffic loop (edge load).